第百三十一號

（昭和十年十一月發行）

抄　錄

後緣の切り取りが翼の空氣力學的特性に及ぼす影響

岡　本　哲　史

本報告は切り欠きのある翼の空氣力學的特性に關する系統的研究の第二報告で，切り欠いた切口の整形を檢討したものである．整形の差異に依る翼の性能の差異を解り易くするため，翼の後緣を全翼幅に沿ふて切り取り，その切口を整形して實驗した．整形としては內接圓で丸めたもの，切口の上側の角をおとしたもの，切口の下側の角をおとしたもの，の三種を調べた．孰れの場合に於いても無揚力角は原翼の場合より減少し，從つて切り欠きによる揚力の減小を整形で改良することは出來ない事を知つた．然し抗力及び翼の後ろの渦流は整形によつて，かなり改良し得た．整形として最も適切なものは內接圓で丸味をつけたもので，實際に多く使はれてゐる切口の下側の角をおとす形式のものは翼の後ろの渦流領域を縮少し得る事の外には殆んど利點を見出すことが出來なかつた．然し切り欠いた部分の翼斷面を原翼のものと相似にするか又は之より矢高の大なる翼形を使へば，切り欠きによる揚力の減小を縮少し又抗力も著しく減小し得ると思ふ．

No. 131.

(Published November, 1935.)

On the Effects of Cutting Away the Trailing Edge on the Aerodynamic Characteristics of a Wing.*

By

Tetusi Okamoto, *Kôgakusi*,

Assistant of the Institute.

Abstract.

The present report is the second part of the systematic experiments on the aerodynamic characteristics of the wing with cut-out. In the first report we studied the effects of extending the rectangular cut-out along the span or in the direction of the chord on the wing characteristics with respect to the case in which the cut end is not made fair. And it is of course that if the cut end is made fair the wing characteristics are also affected. In the present report the problem that what form is suitable as the cutaway section is studied. To this purpose the characteristics of the wing whose trailing edge is fully cut away along the span with four kinds of cut end were tested in the 1·5 m wind tunnel at 30 m/s wind velocity with regard to the two different profiles: the Göttingen 593 and 459 wings.

It is concluded that the most suitable form of the four kinds is that which the cut end is made round with the inscribed circle, and it is still better to make the cutaway section similar to the original wing section if it is permitted from construction. And the flow pattern around the wing section whose trailing edge was cut away was obtained photographically in the 30 m × 1·5 m × 1·5 m water tank of the institute.

* Communicated by Prof. Dr. K. Wada.

Contents.

1. Introduction.

In the preceding paper[1] we studied the effects of the rectangular cut-out on the aerodynamic characteristics of the wing concerning the case in which the cut end was not made fair. It is of course that if the cut end is made round the wing characteristics are also affected. Ackeret's experiments[2] on the characteristics of the wing with circular cut-out show that when the cut end is made round the minimum drag coefficient decreases by about twenty-two per cent.

In the practical design of the wing with cut-out it is necessary and important to have acknowledge of not only the effects of its plan form but also those of the cutaway section. However, investigation of the effects of the fairness of the cut end have almost not been performed since Ackeret's experiments. And the problem that what profile is

(1) T. Okamoto, The Experimental Investigation on the Effects of a cut-out on the Wing characteristics. Report of Aero. Res. Inst., Tokyo Imp. Univ. No. 113. 1934.

(2) Ergebnisse der Aerodynamischen Versuchsanstalt zu Göttingen. Lief. III. pp. 92~94.

suitable as the cutaway section is left to be solved. To this purpose the present paper studied the effects of the fairness of the cut end with respect to the wing whose trailing edge was cut away along the full span, from whose results the most suitable profile as the cutaway section of the wing with cut-out was determined.

2. Range of the tests.

Although the effects of the cutaway section should be tested with regard to the wing with rectangular cut-out, they were, at the present tests, tested regarding the wing whose trailing edge was cut away along the full span by the reasons of convenience in applicating the theory and easiness of discussing the results.

Wings with the four kinds of cut end shown in Fig. 1 were tested in the wind tunnel with regard to the two different profiles: the Göttingen 593 profile whose lower surface is flat and the Göttingen 459 symmetrical profile. And the tests were divided into three parts:

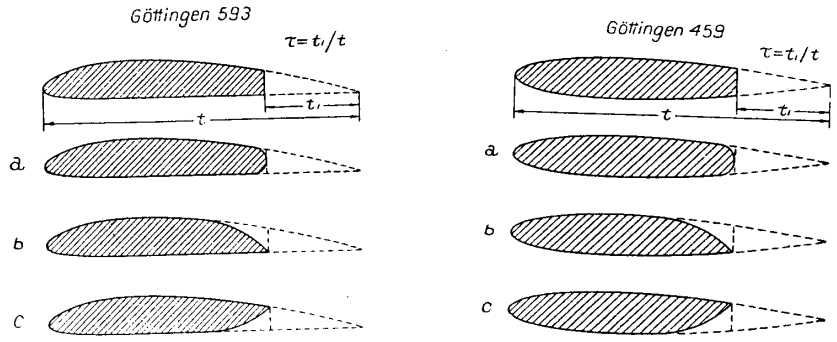

Fig. 1 The cutaway sections tested.

I. The depth of cut-out is changed in the range from the depth-chord ratio $\tau = 0{\cdot}1$ to 0·6 with regard to the case in which the cut end is not made fair.

II. The depth of cut-out is changed in the range from $\tau = 0{\cdot}1$ to 0·4 with respect to the case in which the cut end is made round with the inscribed circle.

III. The comparison of the characteristics of four wings whose cutaway sections are shown in Fig. 1, regarding the case $\tau = 0.3$.

The tests were carried out in the 1·5 m wind tunnel of the institute at the wind velocity of about 30 m/s which corresponded to Reynolds' number of about $3 \cdot 10^5$, the lift and drag having been measured at about 2° intervals of angle of incidence from about $-18°$ and $+24°$.

The original or normal wing is the rectangular whose chief dimensions are as follows:

Span = 75 cm, chord length = 15 cm, aspect ratio = 5 and wing area = 1125 cm^2.

3. Calculation of the coefficients.

Results of the measurements have been reduced to the following coefficient forms.

(i) Lift coefficient and drag coefficient. The lift and drag coefficients based on the wing area of the original wing have been obtained by the equations

$$c_z = \frac{F_z}{qS} \quad \text{and} \quad c_x = \frac{F_x}{qS} - \Delta c_x ,$$

where F_z, c_z the lift, and the lift coefficient,

F_x, c_x the drag (not corrected for the interference of the tunnel wall), and the drag coefficient,

S the wing area of the original aerofoil,

q dynamic pressure,

Δc_x correction of the drag coefficient for the interference of the tunnel wall.

The angle of incidence (α) and the drag have been corrected for the effect of the tunnel wall. Namely,

$$\Delta c_x = 0.00796\, c_z^2 ,$$
$$\Delta \alpha = 0.456\, c_z \qquad \text{(degree)}.$$

The lift and drag coefficients based on the actual wing area (S') have been expressed in the following forms

$$c_z' = \frac{F_z}{qS'} = c_z \frac{1}{1-\tau} \quad \text{and} \quad c_x' = \frac{F_x}{qS'} - \Delta c_x' = c_x \frac{1}{1-\tau} .$$

(ii) Moment coefficient and centre of pressure coefficient. These coefficients based on the wing area and chord length of the original aerofoil have been calculated by the equations

$$c_m = \frac{M}{qSt} \quad \text{and} \quad c_p = \frac{s}{t} = \frac{-c_m}{c_z \cos\alpha + c_x \sin\alpha} ,$$

where M, c_m the moment about the leading edge, and the moment coefficient,

c_p the centre of pressure coefficient,

t the chord length of the original wing,

s the distance of the centre of pressure behind the leading edge.

The moment has been considered to be positive when it tends to raise the leading edge of the wing.

The moment coefficient and the centre of pressure coefficient based on the actual wing area (S') and the actual chord length (t') have been expressed by the following equations

$$c_m' = \frac{M}{qS't'} = c_m \frac{1}{(1-\tau)^2} , \quad \text{and} \quad c_p' = \frac{s}{t'} = c_p \frac{1}{1-\tau} .$$

4. Results of the wind tunnel tests on the Göttingen 593 wing[3]

I. *The cut end is not made fair.*

The effects of cutting away the trailing edge on the wing characteristics in the case in which the cut end is not made round have been

(3) The data of the tests have been listed in tables in the Journal of Aero. Res. Inst., Tokyo Imp. Univ. No. 125. 1935. p. 60.

already investigated by J. Ackeret[4] with regard to the Göttingen 460 and 508 profiles, the depth of cut-out having been changed in the range from $\tau = 0.1$ to 0·7, and M. Ono[5] also has studied this problem for the case in which the depth of cut-out was not so large. And therefore these effects have been discussed sufficiently, but these tests, which were made about ten years ago, have more or less irregularities or inaccuracies in the results of measurement and thus inconvenience takes often place in the analysis. By such reasons and because these tests will be the foundation of the future investigation the similar tests are now repeated.

The model wings used in the tests are shown in Fig. 2. and the depth of cut-out is changed in the range from $\tau = 0.1$ to 0·6. The results of the tests are presented in figures from 8 to 17.

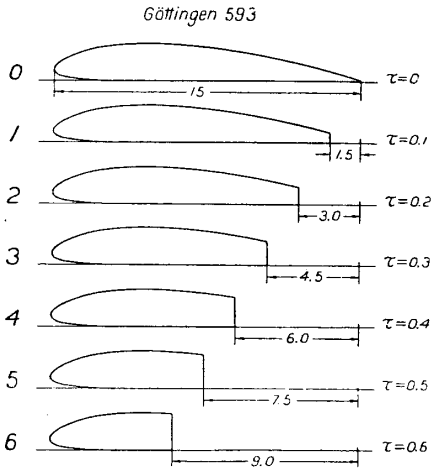

Fig. 2. The model wings. The span is 75 cm for all wings.

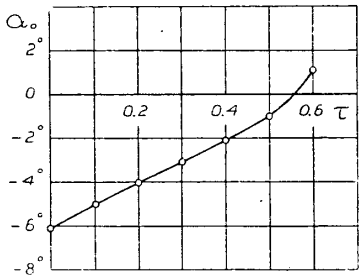

Fig. 3. Variation of the angle of zero lift with the depth-chord ratio τ.

(i) *Lift coefficient.* The lift coefficient based on the original wing area is plotted against the angle of incidence in Fig. 8. The slope of

(4) Ergebnisse der Aerodynamischen Versuchsanstalt zu Göttingen. Lief. III. p. 82.
(5) M. Ono, Jour. of Aero. Res. Inst., Tokyo Imp. Univ. No. 26. 1926. p. 115.

the lift curve or $\frac{dc_z}{da}$ decreases with the depth of cut-out. Denoting the slope of the lift curve of the original wing and of the wing whose trailing edge is cut away with $\bar{c}$ and c respectively, we have the following empirical equation

$$L = \frac{c}{\bar{c}} = 1 - 1{\cdot}55\,\tau^2 + 0{\cdot}45\,\tau^3. \qquad (1)$$

The angle of incidence (α_0) for zero lift decreases linearly with the depth of cut-out in the limit $\tau \leqq 0{\cdot}5$, as is shown in Fig. 3, and in this limit the connection of α_0 the angle of zero lift with τ the depth-chord ratio can be written in the form

$$\alpha_0 = \bar{\alpha}_0 (1 - 1{\cdot}64\,\tau)\,, \qquad (2)$$

where $\bar{\alpha}_0$ is the angle of zero lift of the original wing.

And now we can obtain the empirical formula which estimates the lift coefficient in the limit $\tau \leqq 0{\cdot}5$. When the angle of incidence is quitely small, the lift coefficient is generally written in the form

$$c_z = c\,(\alpha - \alpha_0)\,, \qquad (3)$$

and for the original wing

$$\bar{c}_z = \bar{c}\,(\alpha - \bar{\alpha}_0)\,. \qquad (3a)$$

Substituting the equations (1) and (2) in the equation (3) and supposing the equation (3 a), we have the following empirical formula

$$c_z = (\bar{c}_z - \bar{c}_{z_0} n)\,L\,, \qquad (4)$$

where $n = 1{\cdot}64\,\tau$ and $\bar{c}_{z_0}$ denotes the lift coefficient of the original wing at zero angle of incidence. The maximum lift coefficient decreases with the depth of cut-out, as is shown in Fig. 4, and the stalling angle increases with increasing the depth of cut-out.

The lift coefficient based on the actual wing area is plotted against the angle of incidence in Fig. 14. In this case the slope of the lift curve increases with the depth of cut-out, and this increment depends partely upon the increase of the aspect ratio of the wing which is $\bar{a}/(1-\tau)$, where $\bar{a}$ is the aspect ratio of the original wing. The maximum lift coefficient based on the actual wing area increases, on the contrary to the above case, with the depth of cut-out, as is shown in Fig. 4.

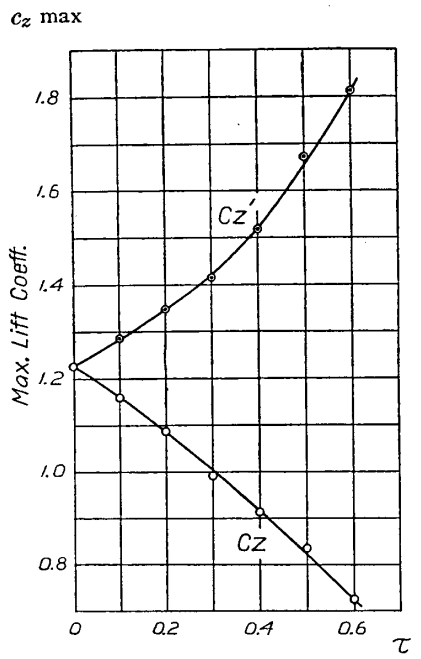

Fig. 4. Variation of the maximum lift coefficient with the depth-chord ratio τ. c_z is based on the original wing area, and c_z' based on the actual one.

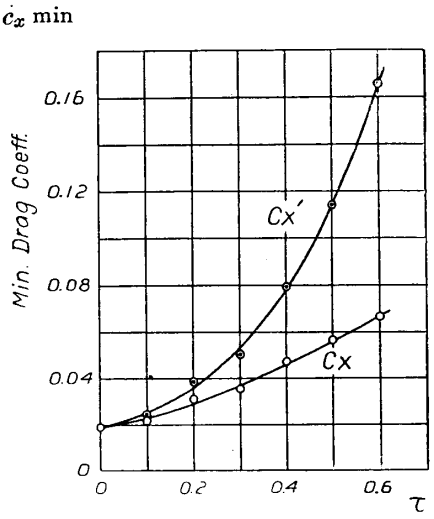

Fig. 5. Variation of the minimum drag coefficient with the depth-chord ratio τ. c_x is based on the original wing area, and c_x' based on the actual one.

(ii) *Drag coefficient.* The drag coefficient based on the original wing area is plotted against the angle of incidence in Fig. 9. At small angles of incidence the drag coefficient increases with the depth of cut-out, but it increases, on the contrary, at larger angles of incidence. The minimum drag coefficient increases with the depth of cut-out, as is shown in Fig. 5.

The drag coefficient based on the actual wing area, which is plotted against the angle of incidence in Fig. 15, increases remarkably with the depth of cut-out.

(iii) *Moment coefficient and centre of pressure coefficient.* The moment coefficient based on the wing area and chord length of the original wing decreases with increasing the depth of cut-out, as is shown in Fig. 10. The centre of pressure coefficient also decreases with the depth of cut-out as is shown in Fig. 11. The variation of the centre of pressure coefficient at $+10^\circ$ angle of incidence with the depth-chord ratio is illustrated in Fig. 6, which indicates that the coefficient based on the original chord length decreases with τ, but that based on the actual chord length increases conversely.

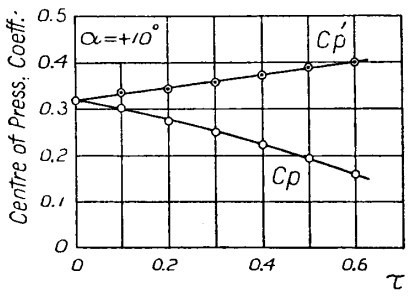

Fig. 6. Variation of the centre of pressure coefficient at $+10^\circ$ angle of incidence with the depth-chord ratio τ. c_p is based on the original chord length and c_p' based on the actual one.

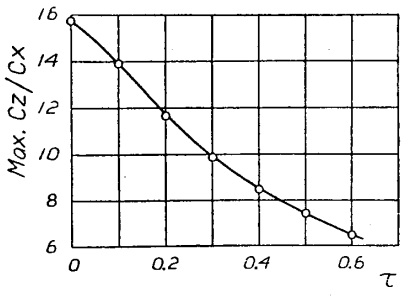

Fig. 7. Variation of the maximum value of the lift-drag ratio with the depth-chord ratio τ.

(iv) *Lift-drag ratio.* The lift-drag ratio is plotted against the angle of incidence in Fig. 12. At the small angles of incidence it decreases with the depth of cut-out. The maximum lift-drag ratio decreases with the depth-chord ratio, as is shown in Fig. 7 and the angle of incidence at which the maximum lift-drag ratio occurs increases with increasing the depth of cut-out.

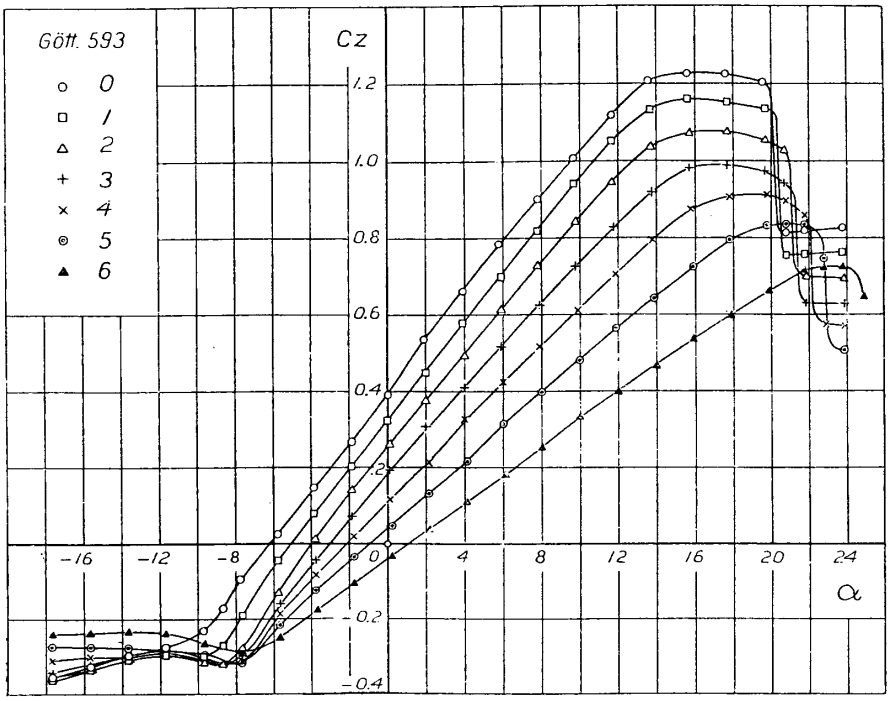

Fig. 8. Curves of the lift coefficient based on the original wing area.

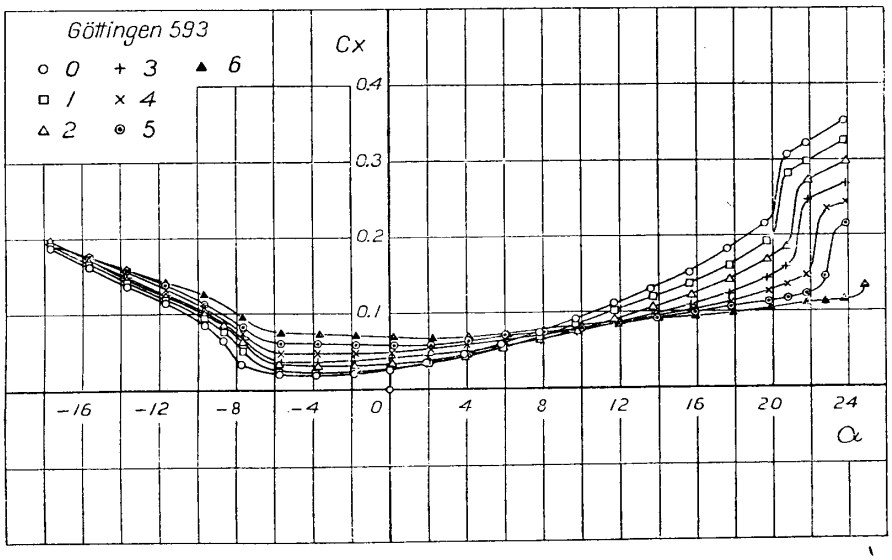

Fig. 9. Curves of the drag coefficient based on the original wing area.

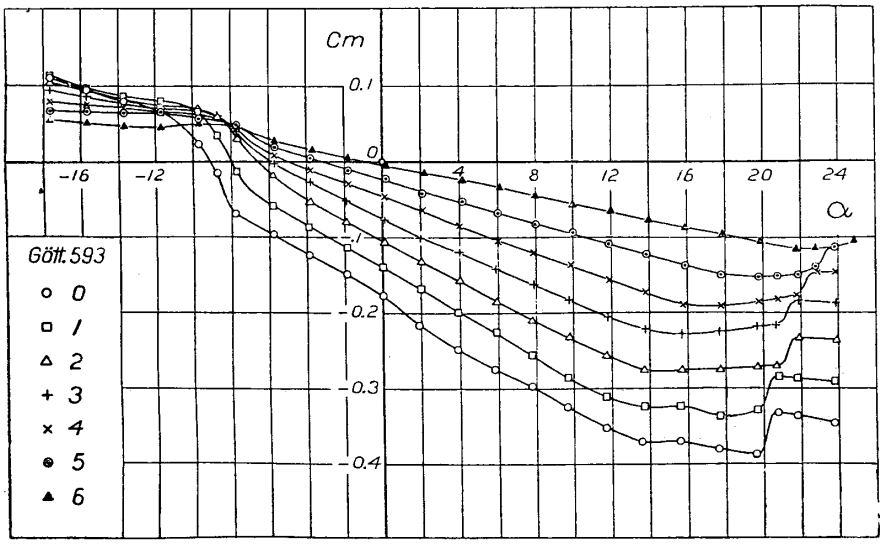

Fig. 10. Curves of the moment coefficient based on the wing area and chord length of the original wing

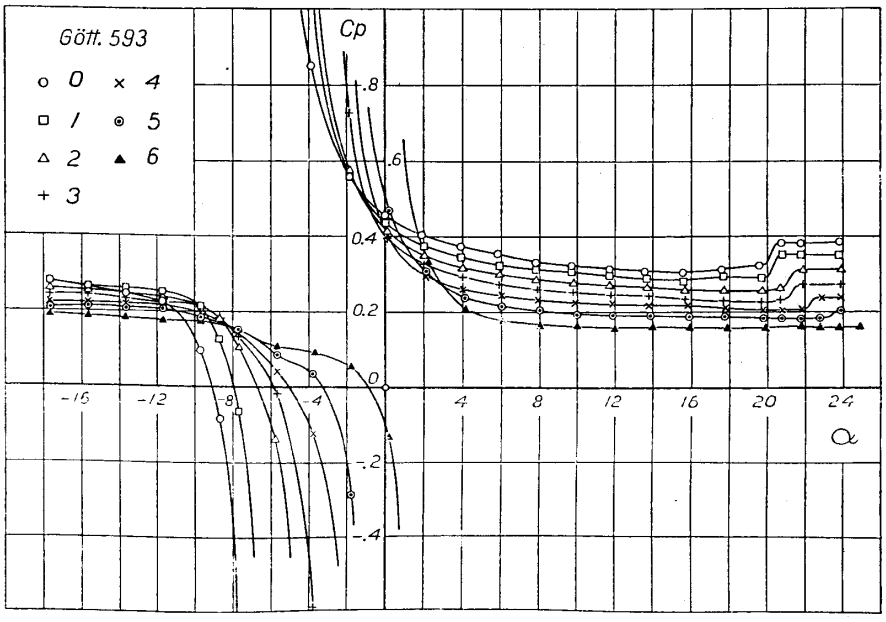

Fig. 11. Curves of the centre of pressure coefficient based on the chord length of the original wing.

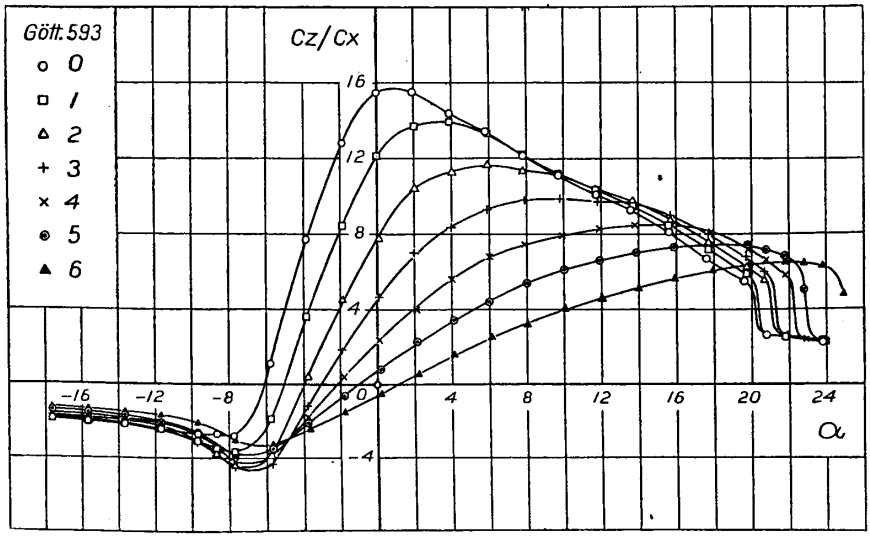

Fig. 12. Curves of the lift-drag ratio.

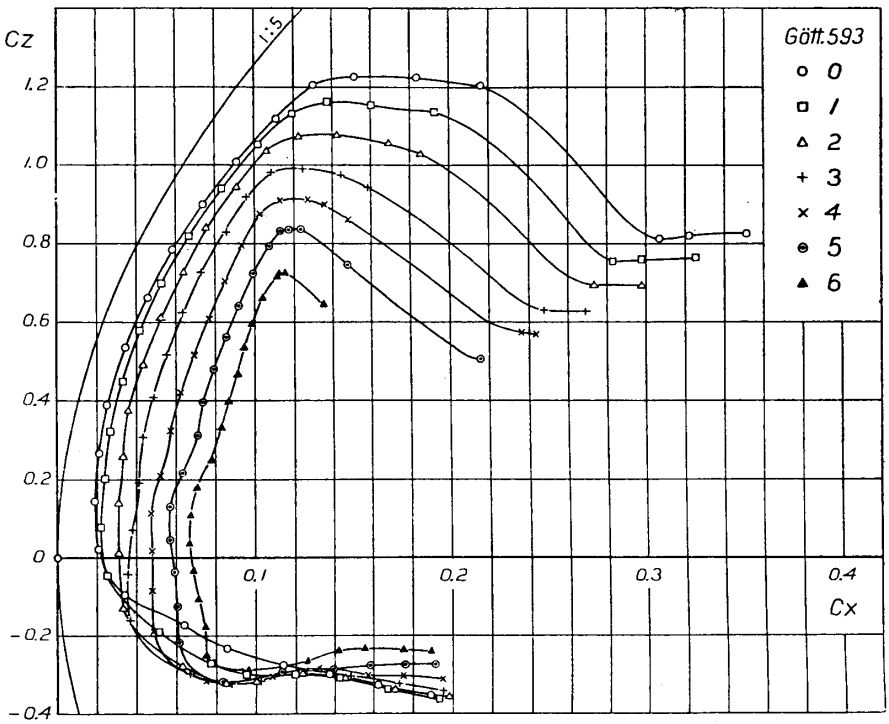

Fig. 13. Polar curves. The coefficients are based on the original wing area.

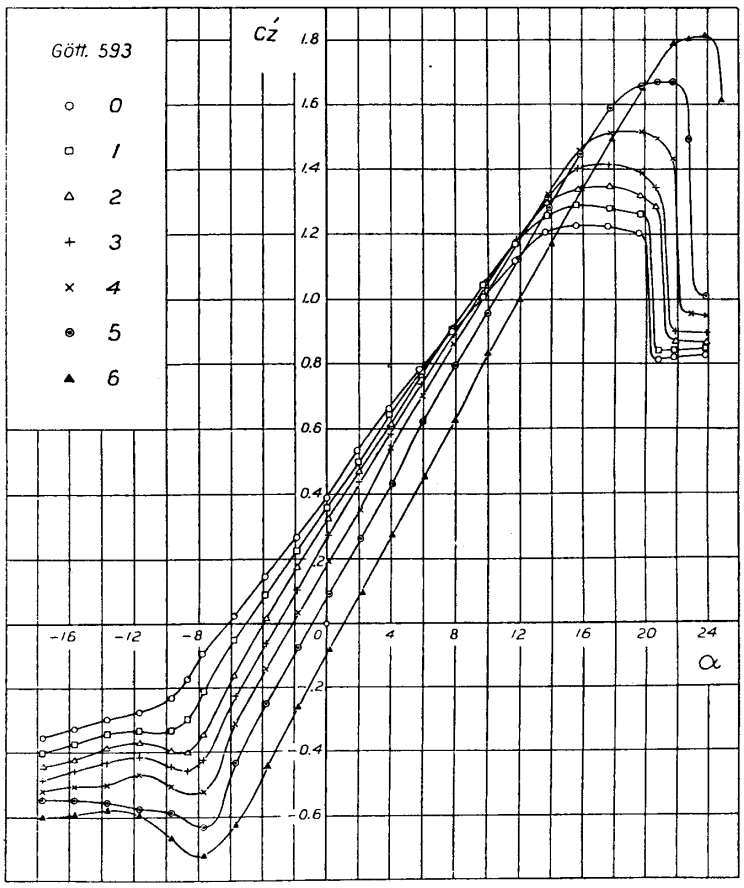

Fig. 14. Curves of the lift coefficient based on the actual wing area.

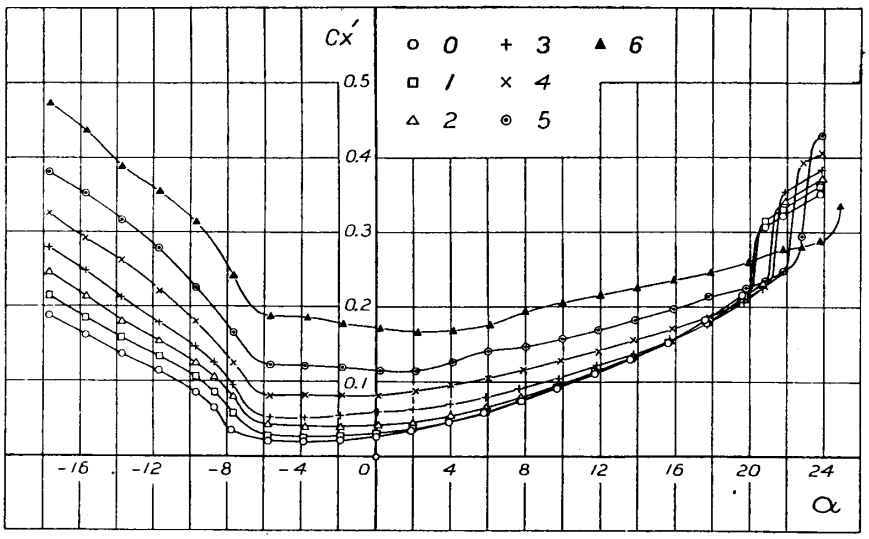

Fig. 15. Curves of the drag coefficient based on the actual wing area.

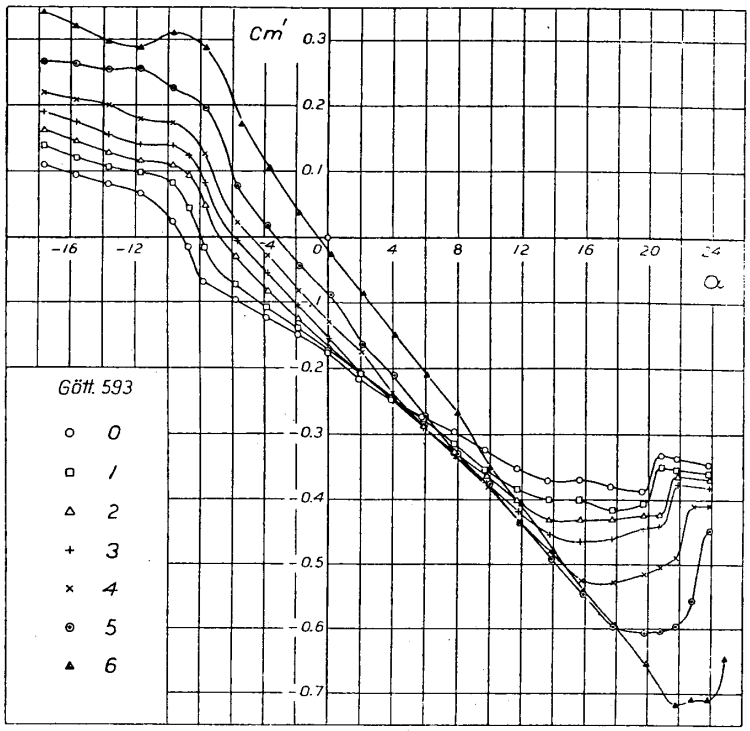

Fig. 16. Curves of the moment coefficient based on the actual wing area and chord length.

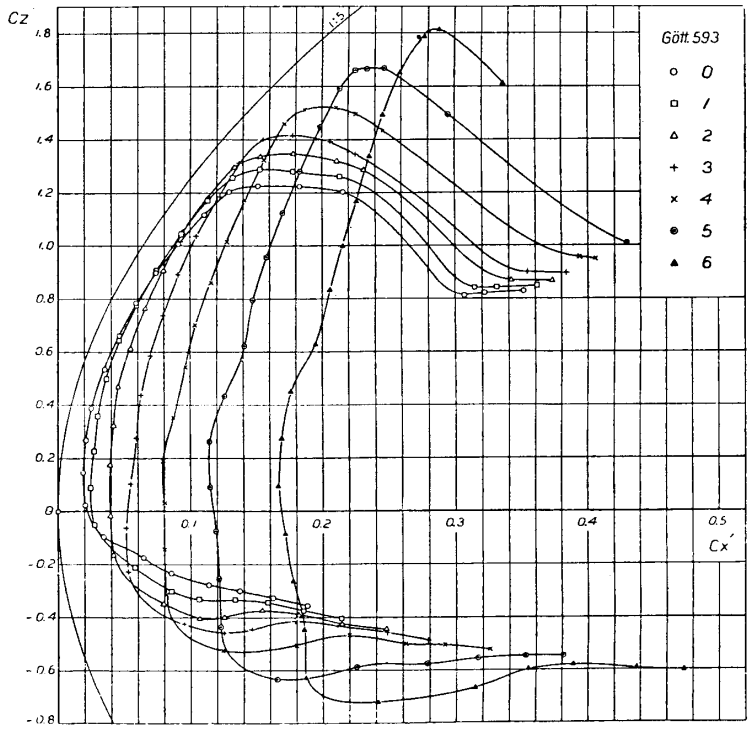

Fig. 17. Polar curves. The coefficients are based on the actual wing area.

II. *The cut end is made round with the inscribed circle.*

Next tests were made with repect to the case in which the cut end is made round with the inscribed circle. The depth of cut-out is changed in the range from the depth-chord ratio $\tau = 0{\cdot}1$ to $0{\cdot}4$, the case of $\tau = 0{\cdot}05$ being added because it will usually utilized to the section for propeller. Moreover, from the results of these tests we can also know the effects of the radius of the trailing edge on the aerodynamic characteristics of the wing.

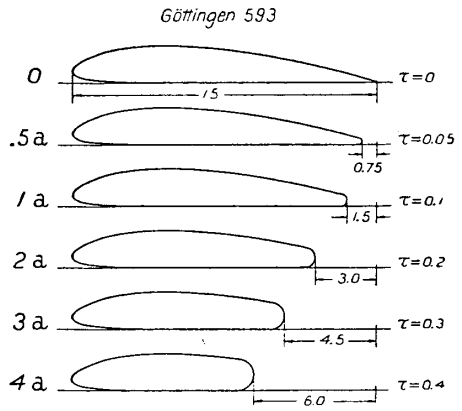

Fig. 18. The model wings. The span is 75 cm for all wings.

The model wings used in the tests are shown in Fig. 18, and the results of the tests are plotted in figures from 24 to 33.

(i) *Lift coefficient.* The lift coefficient based on the original wing area is plotted against the angle of incidence in Fig. 24. The comparison of the curves of the lift coefficient in this case with those in the preceding case is illustrated in Fig. 19. It indicates that if the cut end is made round the maximum lift coefficient and the lift coefficient near the angle of zero lift decrease still more as compared with the case in which the cut end is not made fair. Fig. 20 shows the variation of the maximum lift coefficient with the depth-chord ratio, where the dotted curves denotes the values of the wing without fairness in the cut end.

The lift coefficient based on the actual wing area is plotted against the angle of incidence in Fig. 30. The slope of the lift curve and the maximum lift coefficient increase with increasing the depth of cut-out in the similar manner as the results of the preceding tests.

When the trailing edge is cut away at 95 per cent of chord length in order to obtain the section for propeller, the angle of zero lift decreases

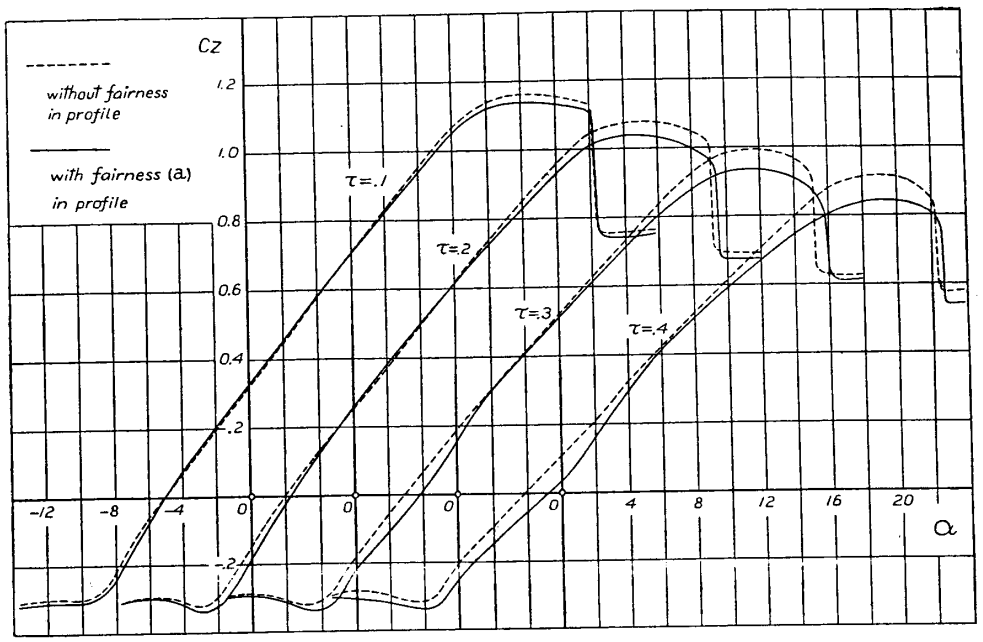

Fig. 19. Comparison of the curve of the lift coefficient of the wing whose cut end is made round with that of the wing without fairness in the cut end.

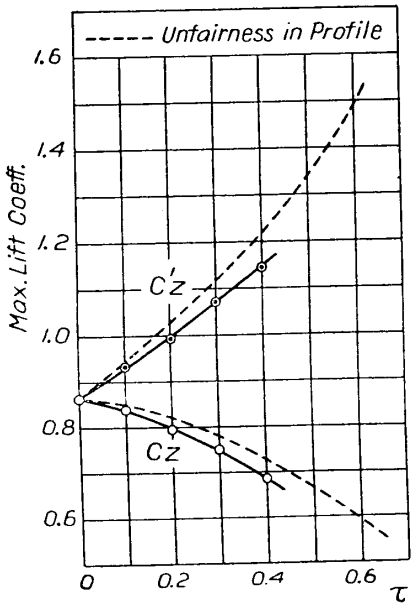

Fig. 20. Variation of the maximum lift coefficient with the depth-chord ratio τ. c_z is based on the original wind area, and c_z' based on the actual one.

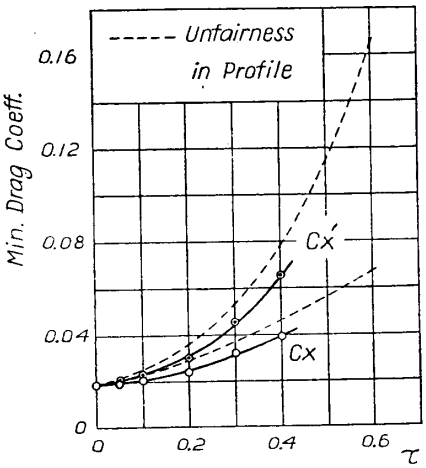

Fig. 21. Variation of the minimum drag coefficient with the depth-chord ratio τ. c_x is based on the original wing area, and c_x' based on the actual one.

by about 10 per cent and the maximum lift coefficient increases by 1·2 per cent as compared with the original wing, where the aspect ratio of the wing increases of course to 5·26.

(ii) *Drag coefficient.* The drag coefficient based on the original wing area decreases considerably as compared with that of the wing without fairness in the cut end, as is shown in Fig. 25. And hence the variation of the minimum drag coefficient with the depth-chord ratio is smaller than that of the preceding case as is shown in Fig. 21.

The drag coefficient based on the actual wing area is plotted against the angle of incidence in Fig. 31.

When the trailing edge is cut away at 95 per cent of chord length in order to make the section for propeller, the drag coefficient based on the actual wing area becomes larger than that of the original wing at the negative angle of incidence, and it is nearly the same at the positive angles of incidence up to about 12°.

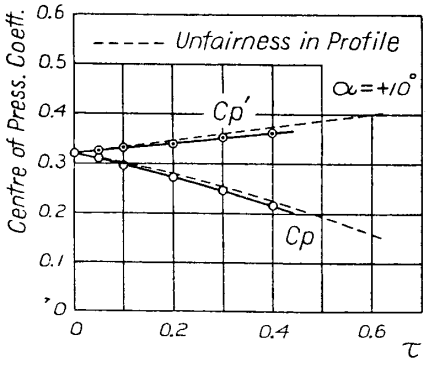

Fig. 22. Variation of the centre of pressure coefficient at +10° angle of incidence with the depth-chord ratio τ. c_p is based on the original chord length, and c_p' based on the actual one.

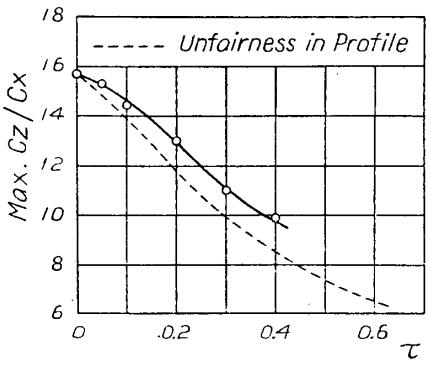

Fig. 23. Variation of the maximum value of the lift-drag ratio with the depth-chord ratio τ.

(iii) *Moment coefficient and centre of pressure coefficient.* The moment coefficient based on the wing area and chord length of the original wing decreases with increasing the depth of cut-out, as is shown in Fig. 26.

The centre of pressure coefficient based on the chord length of the original wing decreases with increasing the depth of cut-out at the relatively large angles of incidence, as is shown in Fig. 27. The variation of this coefficient at $+10^{\circ}$ angle of incidence with the depth-chord ratio is shown in Fig. 22, which indicates that if the cut end is made round the centre of pressure somewhat removes forwards as compared with the case in which the cut end is not made fair.

(iv) *Lift-drag ratio.* The tendency of the variation of the lift-drag ratio with the depth of cut-out is similar as the preceding case, as is shown in Fig. 28. But the value of the lift-drag ratio increases as compared with that of the wing without fairness in the cut end. The maximum value of the lift-drag ratio decreases with increasing the depth of cut-out, as is shown in Fig. 23.

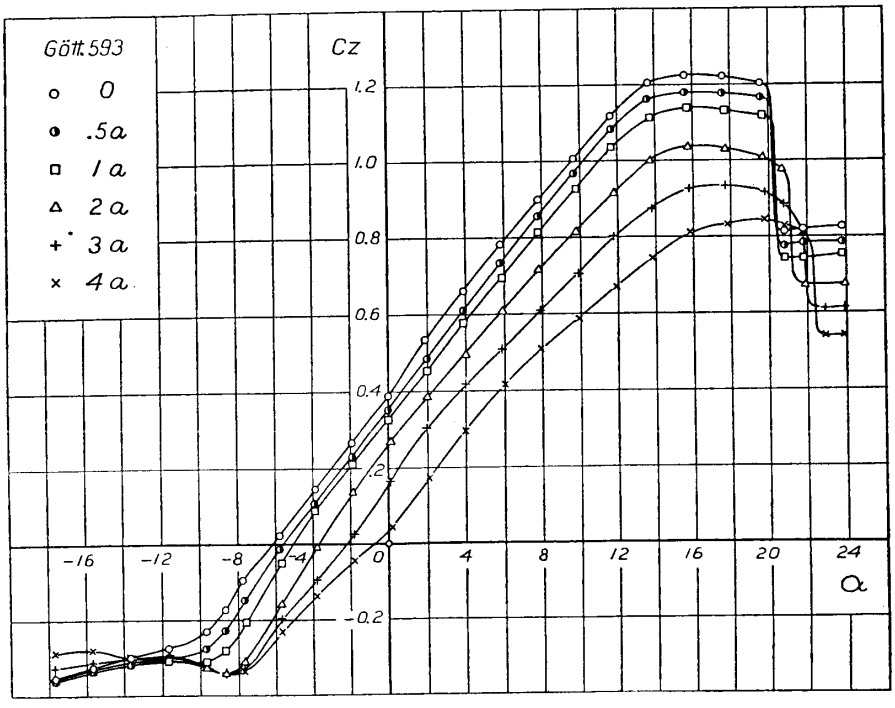

Fig. 24. Curves of the lift coefficient based on the original wing area.

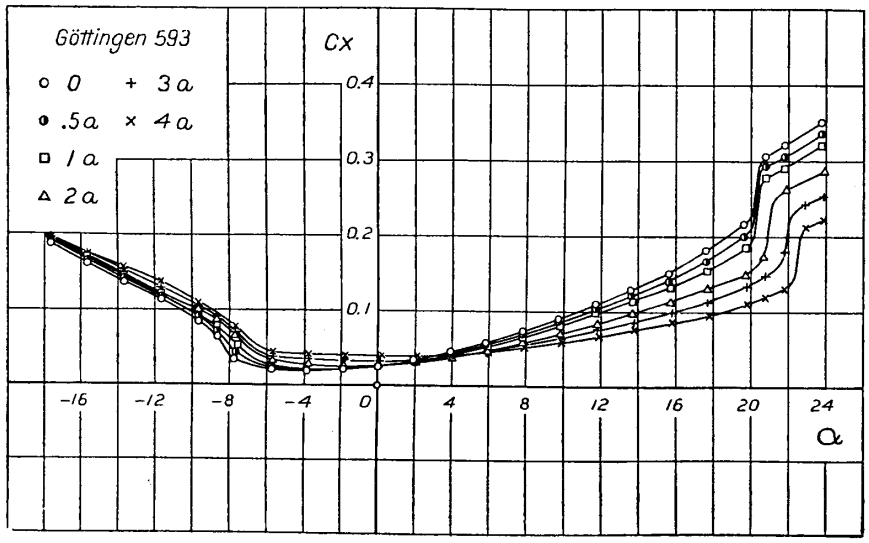

Fig. 25. Curves of the drag coefficient based on the original wing area.

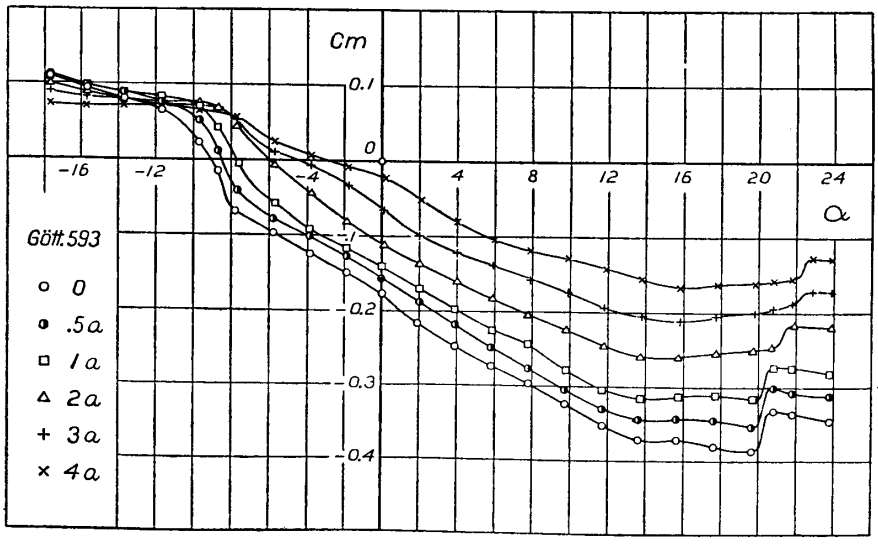

Fig. 26. Curves of the moment coefficient based on the wing area and chord length of the original wing.

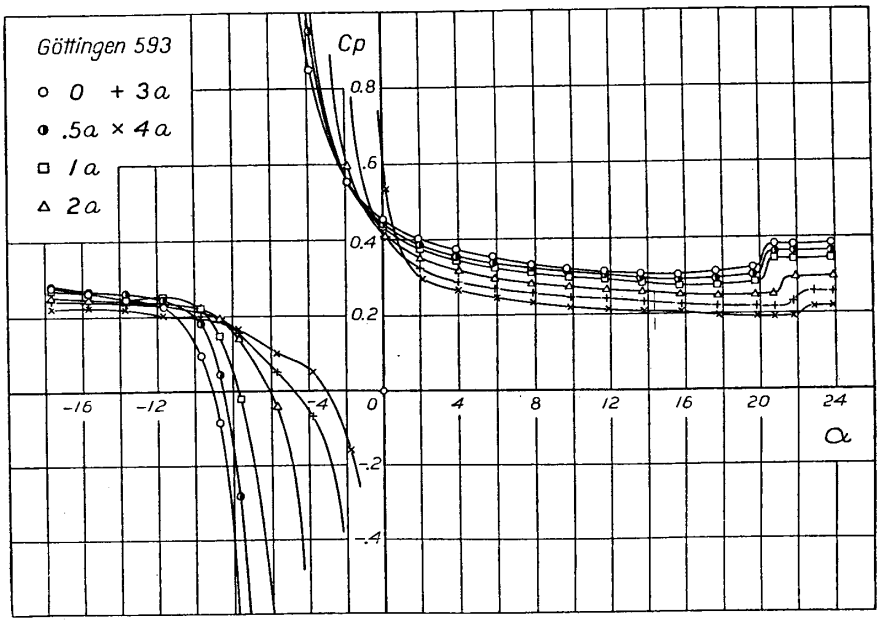

Fig. 27. Curves of the centre of pressure coefficient based on the chord length of the original wing.

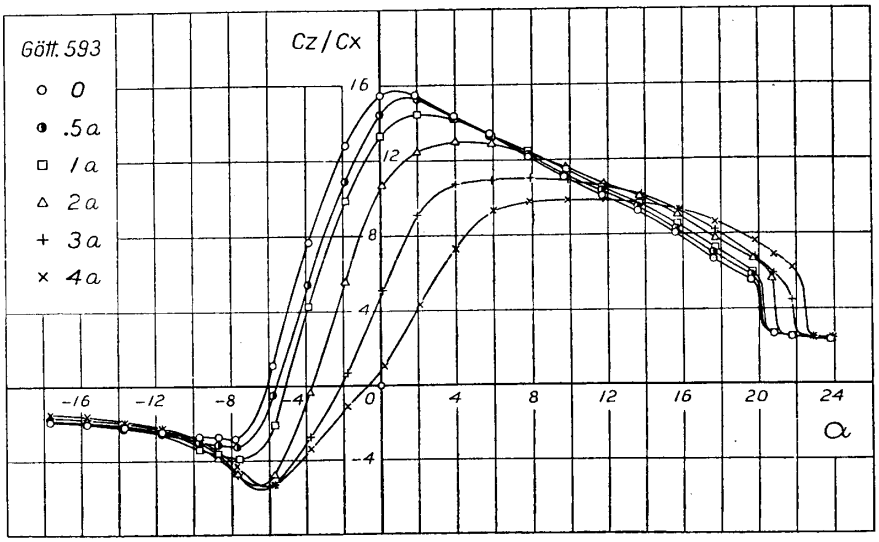

Fig. 28. Curves of the lift-drag ratio.

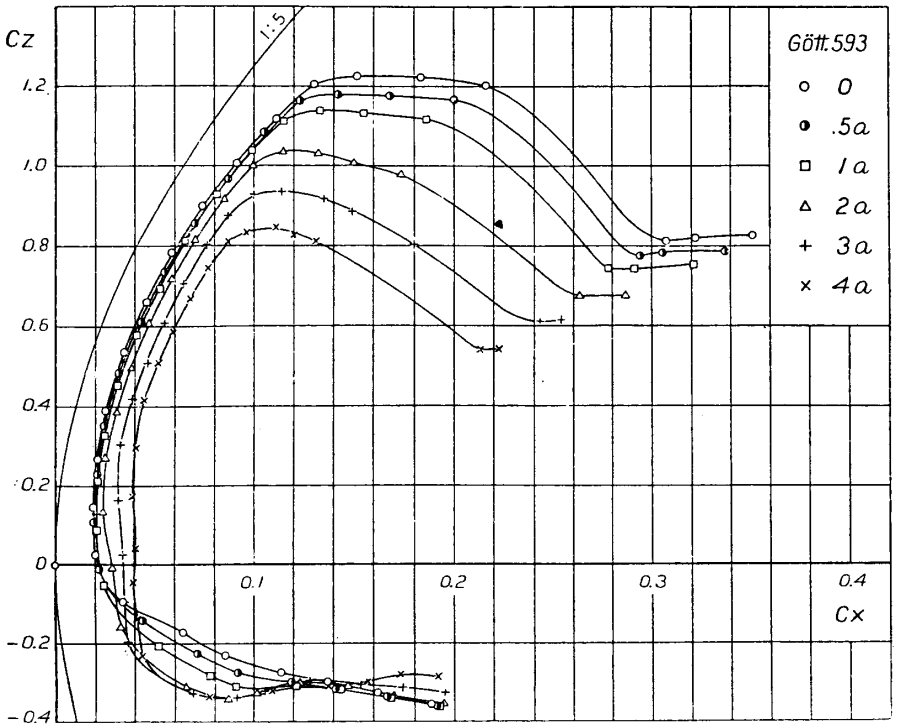

Fig. 29. Polar curves. The coefficients are based on the wing area of the original wing.

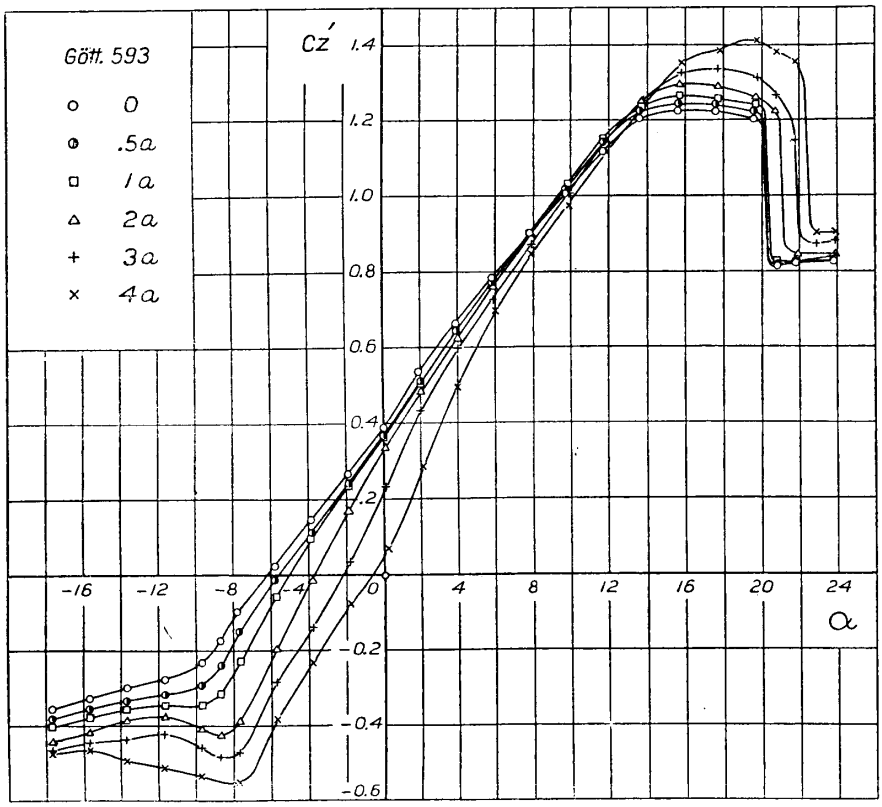

Fig. 30. Curves of the lift coefficient based on the actual wing area.

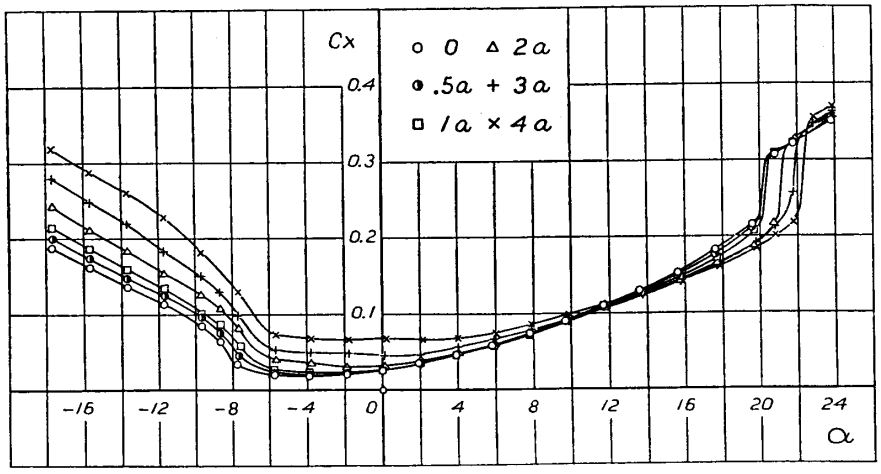

Fig. 31. Curves of the drag coefficient based on the actual wing area.

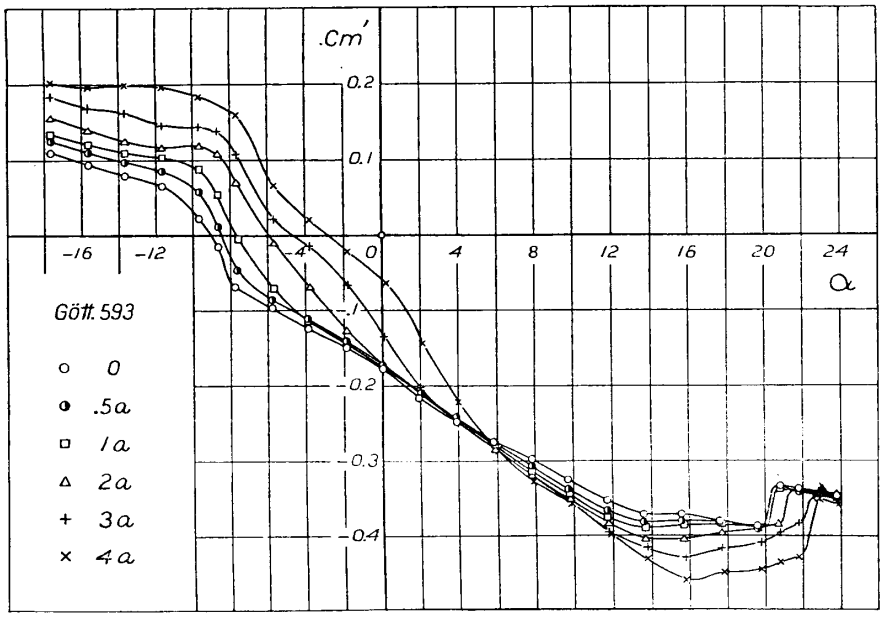

Fig. 32. Curves of the moment coefficient based on the actual wing area and chord length.

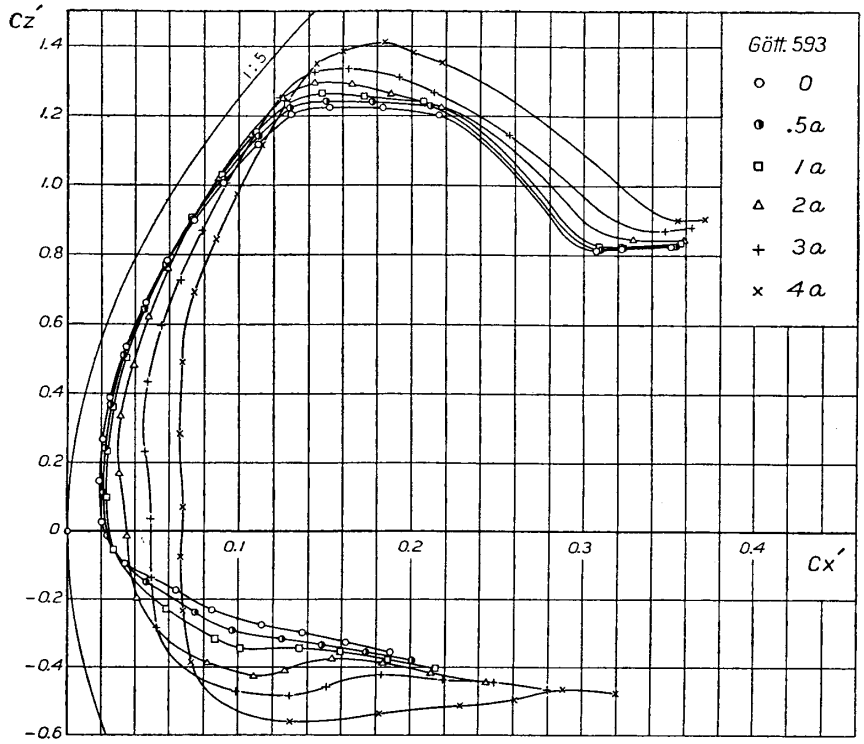

Fig. 33. Polar curves. The coefficients are based on the actual wing area.

III. *Comparison of the characteristics of the wings with various cutaway sections.*

From the preceding tests differences between the aerodynamic characteristics of the wing without fairness and those of the wing whose cut end is made round with the inscribed circle could be known. In the next place the aerodynamic characteristics of the two wings whose sections are designated by 3 *b* and 3 *c* in Figs. 34 and 35 were tested, and by comparing these with the results of the preceding tests the most suitable form as the cutaway section was chosen in the four forms shown in Fig. 34.

The results of the tests are shown in figures from 38 to 43.

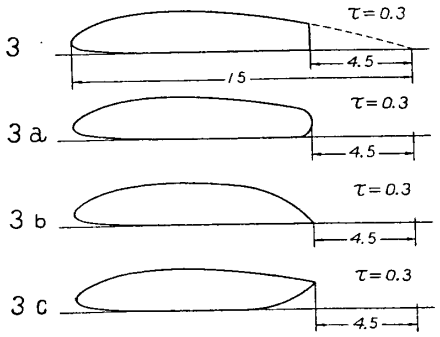

Fig. 34. The model wings. The span is 75 cm for all wings.

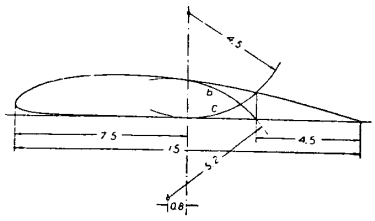

Fig. 35. Details of the 3*b* and 3*c* wings.

(i) *Lift coefficient.* As the present tests were made for purpose of comparing the characteristics of the wings with various cutaway sections, so the discussion on the results was made regarding only the aerodynamic coefficients based on the dimensions of the original wing.

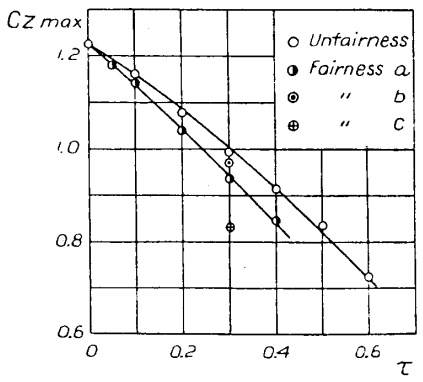

Fig. 36. Variation of the maximum lift coefficient with the fairness in the cut end, plotted against the depth-chord ratio τ.

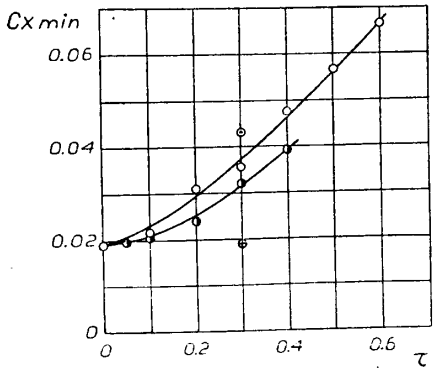

Fig. 37. Variation of the minimum drag coefficient with the fairness in the cut end, plotted against the depth-chord ratio τ.

The lift coefficient is plotted against the angle of incidence in Fig. 38, where the curves for the " 3 " and " 3*a*" wings are brought from the results of the preceding tests.

The lift coefficient of the "3*b*" wing increases so considerably at the angles of incidence from 2° to 13°, that a protuberance occurs on the lift curve. And the maximum lift coefficient increases than that of the "3*a*" wing though it is smaller than that of the wing without fairness in the cut end.

The lift coefficient of the "3c" wing decreases considerably as compared with the other wings and its curve plotted against the angle of incidence has a sudden rise at about +1° angle of incidence, which seems to be led by an abrupt change of the flow past the wing. The comparison of the values of the maximum lift coefficient of these wings is illustrated in Fig. 36.

(ii) *Drag coefficient.* The drage coefficient is plotted against the angle of incidence in Fig. 39. The drag coefficient of the "3*c*" wing is smallest of all and that of the "3*a*" wing is secondly small, and the former increases abruptly at about +1° angle of incidence at which the lift coefficient also increases suddenly. It is to be noticed that the drag coefficient of the "3*b*" wing is larger than that of the "3" wing.

The variation of the minimum drag coefficient with the fairness in cut end is shown in Fig. 37.

(iii) *Moment coefficient and centre of pressure coefficient.* The moment coefficient is plotted against the angle of incidence in Fig. 40. The moment coefficient of the "3*c*" wing is smallest in all and it increases suddenly at about +1° angle of incidence. The curve of the moment coefficient of the "3*b*" wing has a protuberance at the angles of incidence from 2° to 10°.

The centre of pressure coefficient is plotted against the angle of incidence in Fig. 41. The centre of pressure of the "3*b*" wing is slightly behind that of the "3" or "3*a*" wing. And the centre of pressure of the "3*c*" wing is in front of that of any other wing.

(iv) *Lift-drag ratio.* The curves of the lift-drag ratio plotted against the angle of incidence are shown in Fig. 42. The maximum value of

this ratio decreases in order of the "3c", "3b", "3a" and "3" wings. However, the "3a" wing is superior to the other wings with regard to the lift-drag ratio at the angles of incidence occurred usually in flight.

(v) *Conclusions.* When the cut end is made round with the inscribed circle, the lift coefficient somewhat decreases and the drag coefficient also decreases considerably as compared with the wing whose cut end is not made fair, so that the lift-drag ratio is relatively large at the wide range of the angle of incidence.

If the cut end is made fair with the "b" type, the lift coefficient does not so much increase in comparison with the wing whose cut end is not made fair except at angles of incidence from 2° to 12°, although this fairness is expected to give an increase of the lift coefficient or specially the zero lift angle because the camber of the wing section is increased.

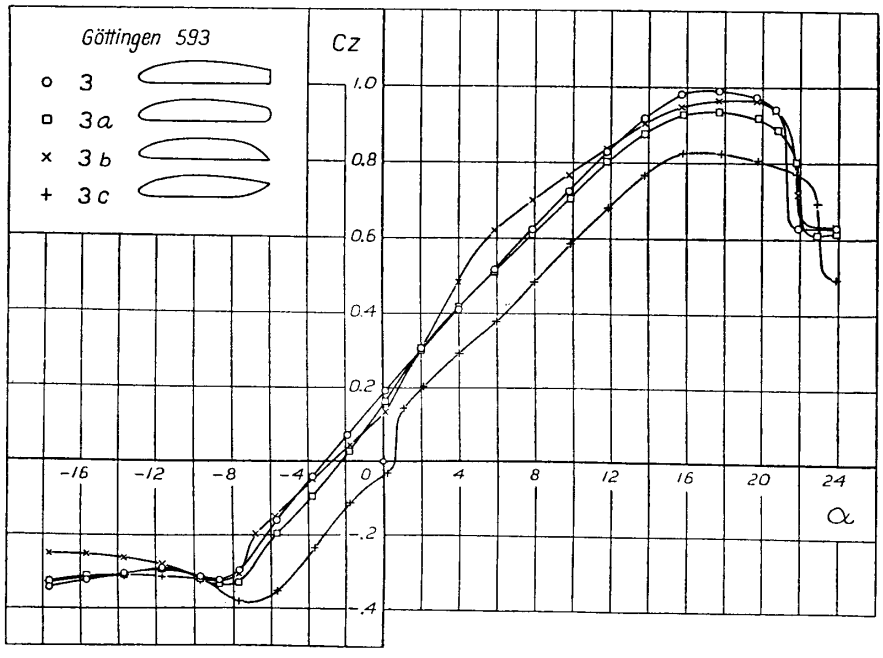

Fig. 38. Curves of the lift coefficient.

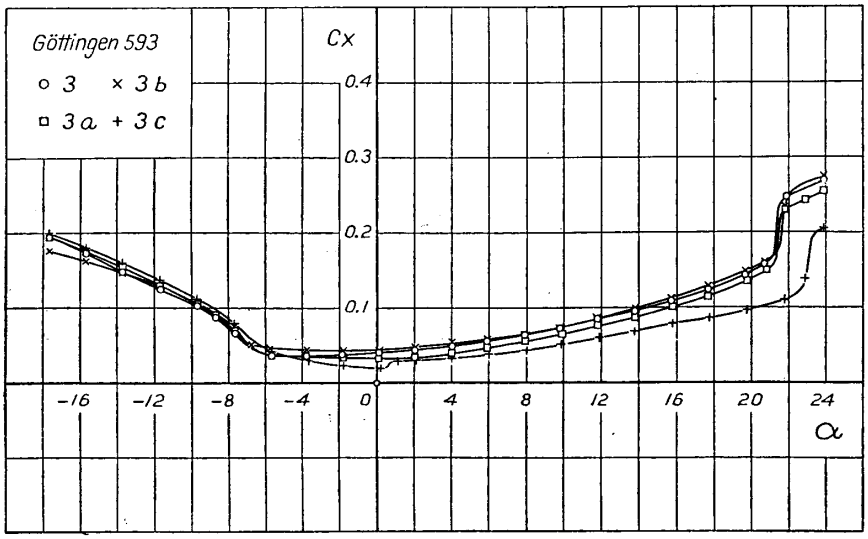

Fig. 39. Curves of the drag coefficient.

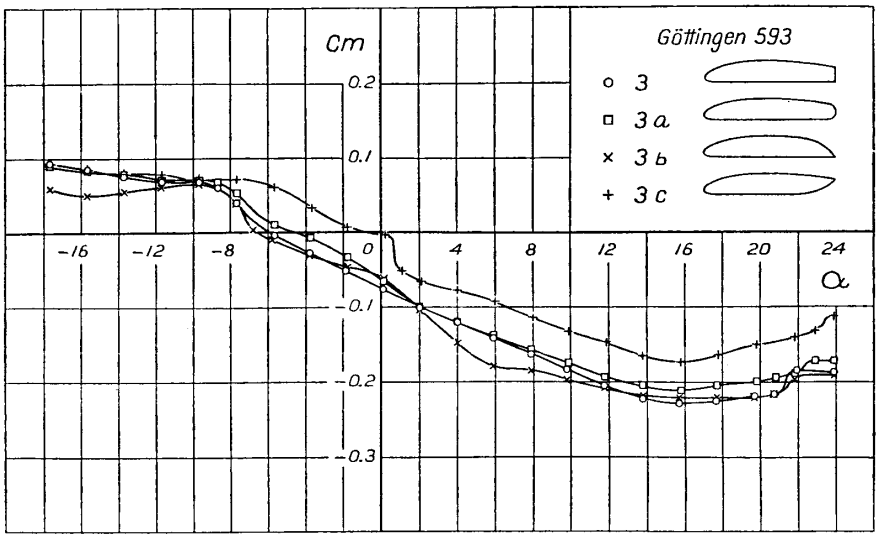

Fig. 40. Curves of the moment coefficient.

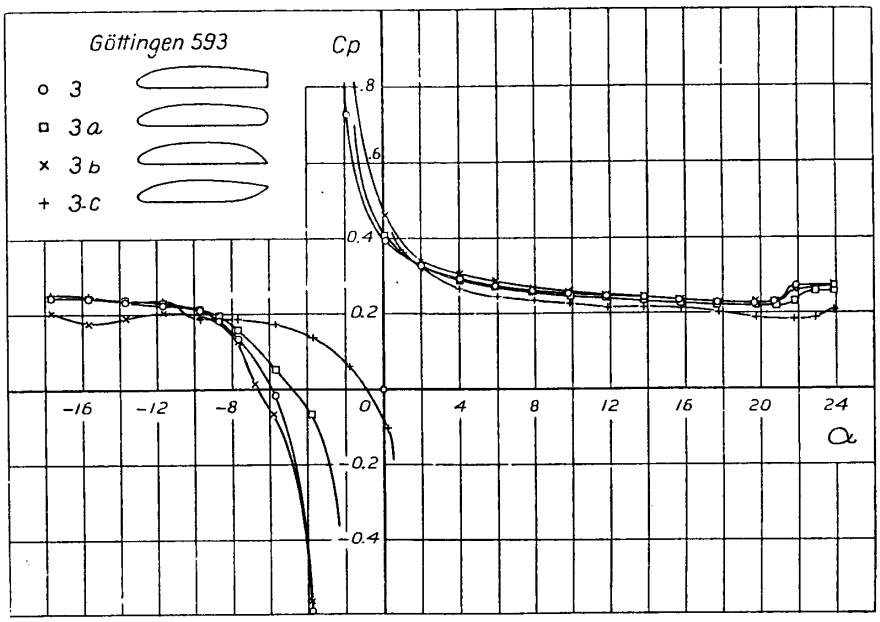

Fig. 41. Curves of the centre of pressure coefficient.

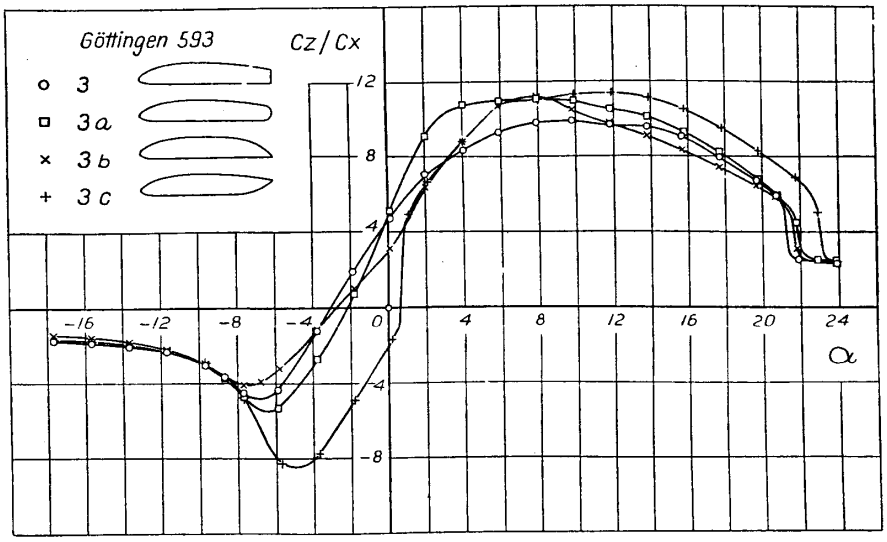

Fig. 42. Curves of the lift-drag ratio.

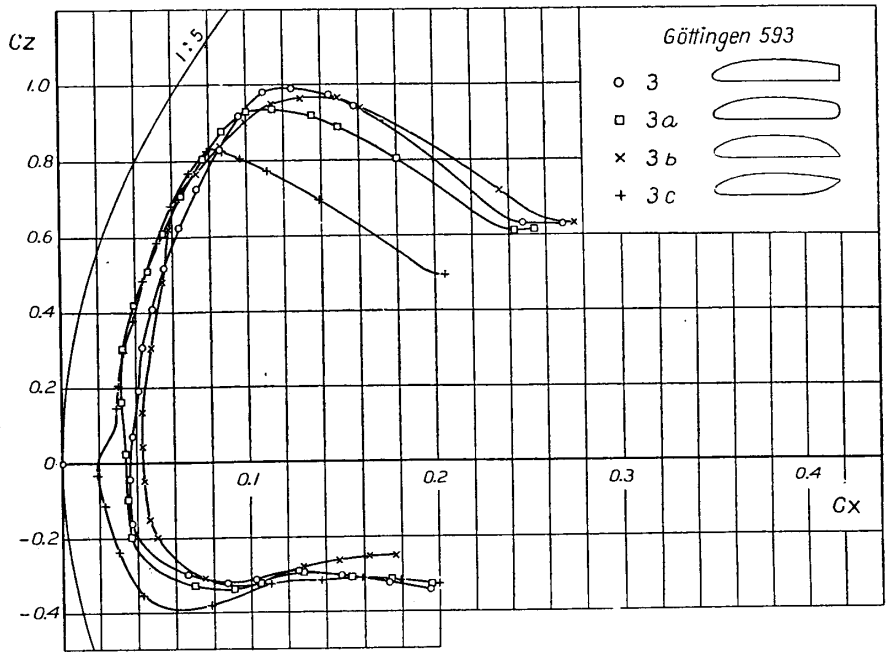

Fig. 43. Polar curves.

When the cut end is made fair with the "*c*" type, the drag coefficient and the lift coefficient likewise decreases considerably. Moreover, in this case it seems to occur a sudden change in the flow around the wing.

From the above discussions it is concluded that the fairness "*a*" which is made with the inscribed circle is the most suitable as the cutaway section in the four forms mentioned.

5. Results of the wind tunnel tests on the Göttingen 459 wing.[6]

It has long been known that the effects of cutting the trailing edge on the wing characteristics varies with the wing section and especially

(6) The data of the tests have been listed in tables in Jour. of Aero. Res. Inst., Tokyo Imp. Univ. No. 132. 1935. p. 630.

with the camber of profile. Now, the same tests as the preceding are carried with regard to the Göttingen 459 symmetrical profile.

I. *The cut end is not made fair.*

The model wings tested are shown in Fig. 44, the depth of cut-out being changed in the range from $\tau = 0{\cdot}1$ to $0{\cdot}6$. Results of the tests are shown in figures from 49 to 58.

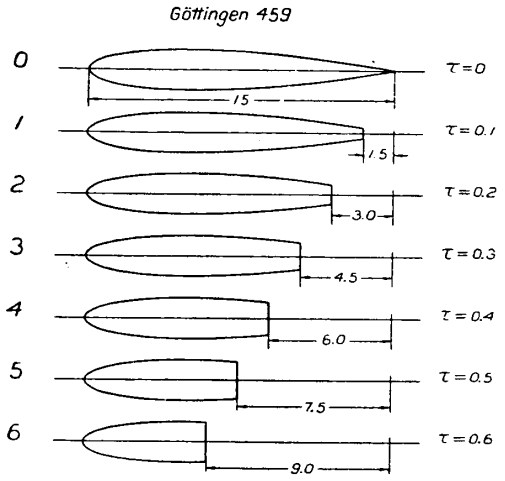

Fig. 44. The model wings. Tee span is 75 cm for all wings.

(i) *Lift coefficient.* The lift coefficient based on the original wing area is plotted against the angle of incidence in Fig. 49. The slope of this lift curve or $\frac{dc_z}{d\alpha}$ decreases continuously with increasing the depth of cut-out and the rate of decrease for this case is the same as for the case of the Göttingen 593 wing, which can be represented by equation (1). It can, thus, be seen that the variation of the value of $\frac{dc_z}{d\alpha}$ with the depth of cut-out is independent of the camber of profile.

The stalling angle increases and the lift coefficient at angles of incidence beyond the stalling angle decreases with increasing the depth of cut-out. The maximum lift coefficient decreases at the smaller rate with the depth of cut-out than for the Göttingen 593 wing, as is shown in Fig. 45. It can, thus, be concluded that the smaller is the camber of profile, the rate of decrease of the maximum lift coefficient with the depth of cut-out becomes smaller.

The lift coefficient based on the actual wing area is plotted against the angle of incidence in Fig. 55. The slope of the lift curve increases

and the maximum lift coefficient also increases with the depth of cut-out, as is shown in Fig. 45.

(ii) *Drag coefficient.* The drag coefficient based on the original wing area is plotted against the angle of incidence in Fig. 50. The drag coefficient increases with the depth of cut-out at angles of incidence below the stalling angle but it decreases at angles beyond the stalling angle. The minimum drag coefficient increases at the greater rate with the depth of cut-out than for the Göttingen 593 wing, as is shown in Fig. 46.

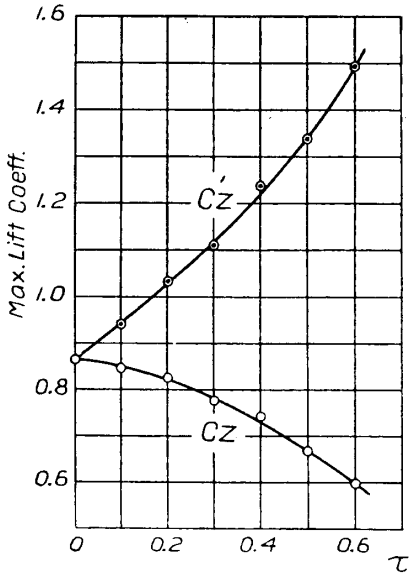

Fig. 45. Variation of the maximum lift coefficient with the depth-chord ratio τ. c_z is based on the original wing area, and c_z' based on the actual one.

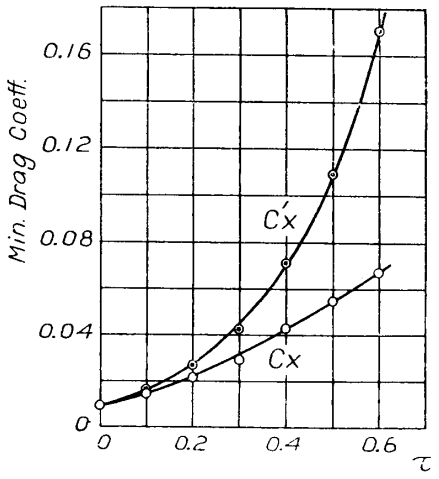

Fig. 46. Variation of the minimum drag coefficient with the depth-chord ratio τ. c_x is based on the original wing area, and c_x' based on the actual one.

The drag coefficient based on the actual wing area, which is shown in Fig. 56, increases strongly with the depth of cut-out both at small angles and at the angles beyond the stalling angle.

(iii) *Moment coefficient and centre of pressure coefficient.* The moment coefficient based on the wing area and chord length of the original wing decreases with the depth of cut-out, but that based on the actual ones increases on the contrary.

The centre of pressure coefficient based on the original chord length decreases with the depth of cut-out, as is shown in Fig. 52. The value of this coefficient at $+10^\circ$ angle of incidence is plotted against the depth-chord ratio τ in Fig. 47, the rate of increase of the value of c_p with τ being slightly smaller than that of the Göttingen 593 wing.

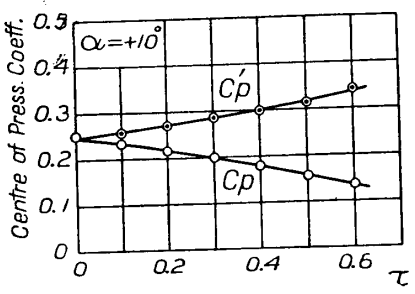

Fig. 47. Variation of the centre of pressure coefficient at $+10^\circ$ angle of incidence with the depth-chord ratio τ. c_p is based on the original chord length and c_p' based on the actual one.

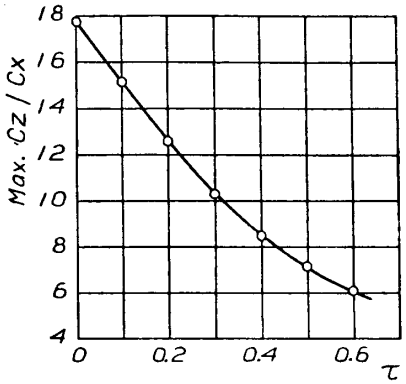

Fig. 48. Variation of the maximum value of the lift-drag ratio with the depth-chord ratio τ.

(iv) *Lift-drag ratio.* The lift-drag ratio, which is plotted against the angle of incidence in Fig. 53, decreases with the depth of cut-out. And the maximum value of the lift-drag ratio decreases at the greater rate with the depth of cut-out than for the Göttingen 593 wing, as is shown in Fig. 48. The angle of incidence at which the maximum value of the lift-drag ratio occurs increases with the depth of cut-out, and it coincides approximately with the stalling angle when the depth of cut-out is sufficiently large.

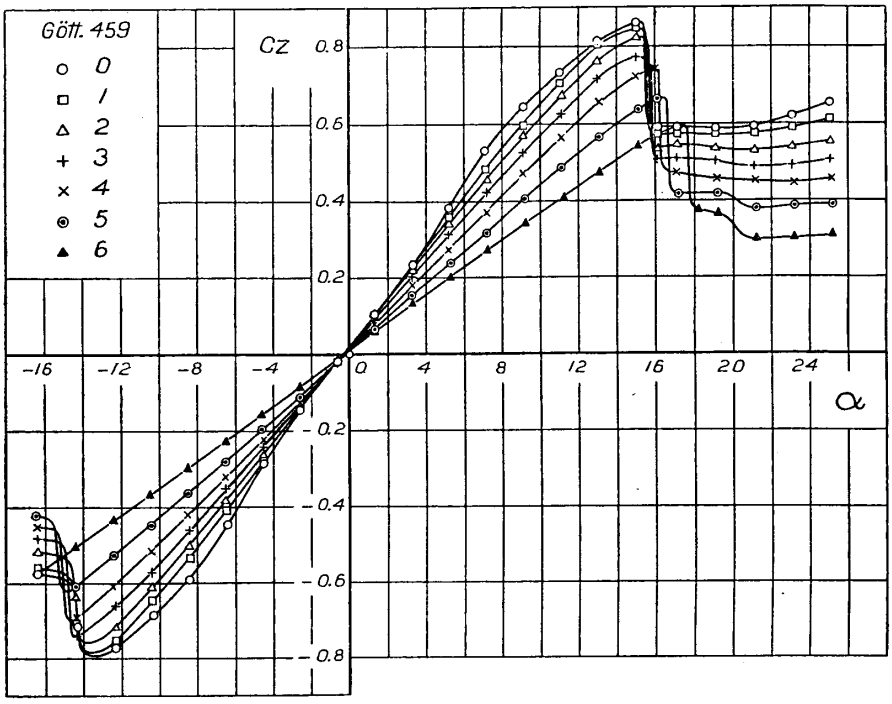

Fig. 49. Curves of the lift coefficient based on the original wing area.

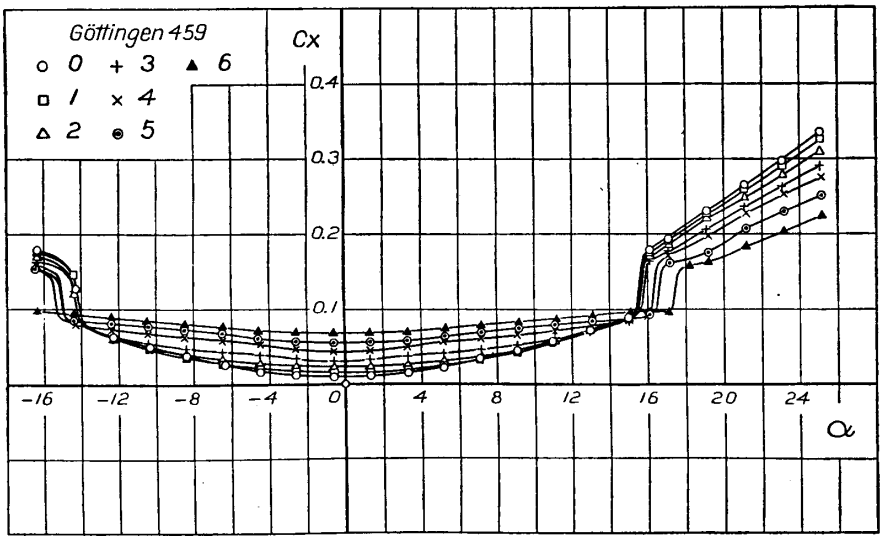

Fig. 50. Curves of the drag coefficient based on the original wing area.

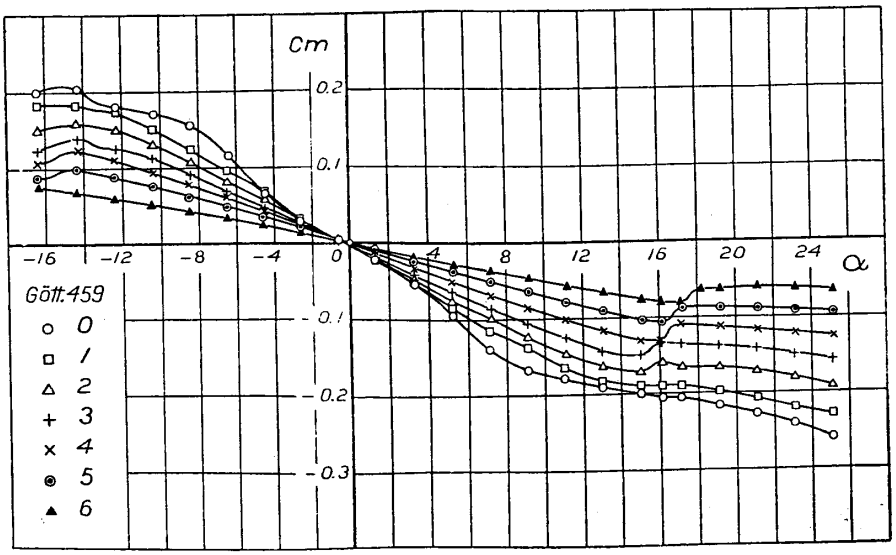

Fig. 51. Curves of the moment coefficient based on the wing area and chord length of the original wing.

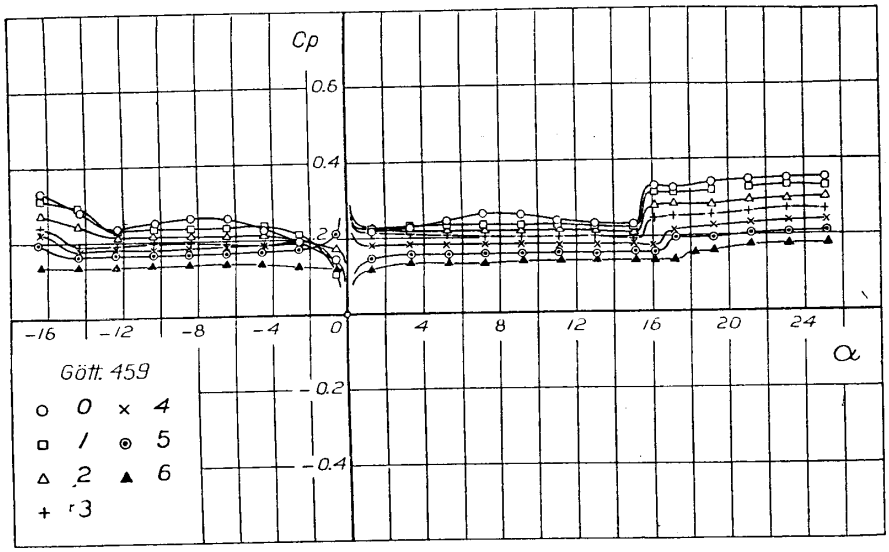

Fig. 52. Curves of the centre of pressure coefficient based on the chord length of the original wing.

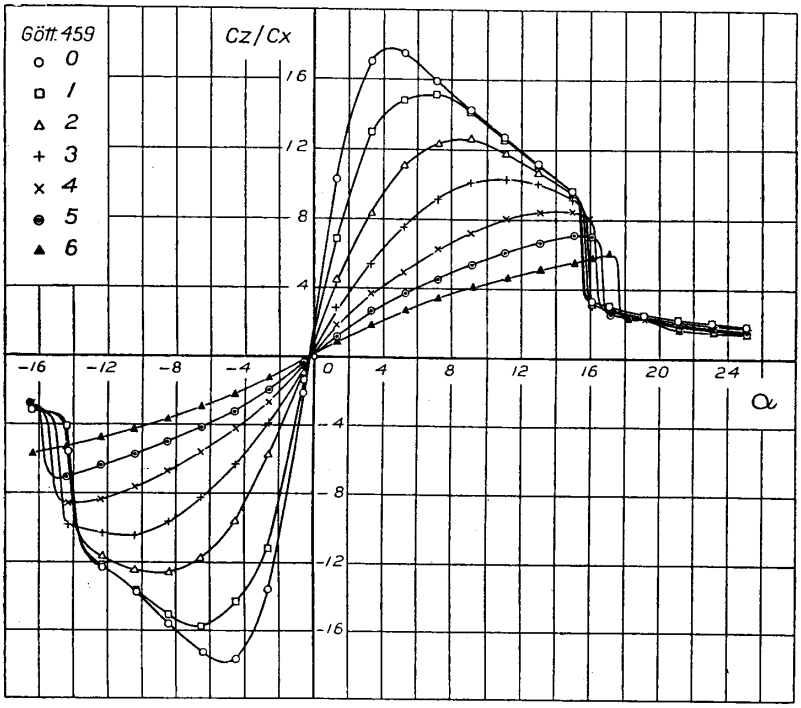

Fig. 53. Curves of the lift-drag ratio.

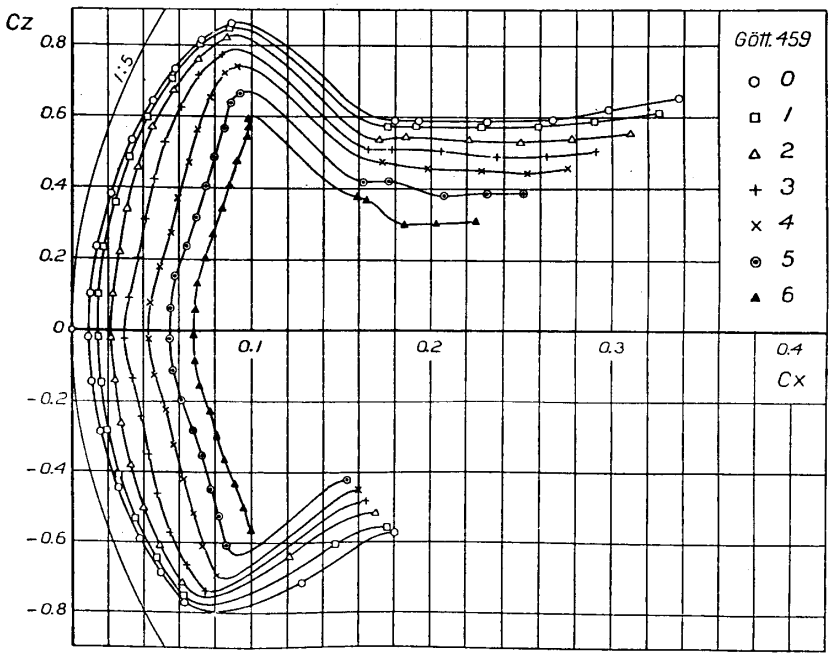

Fig. 54. Polar curves. The coefficients are based on the actual wing area.

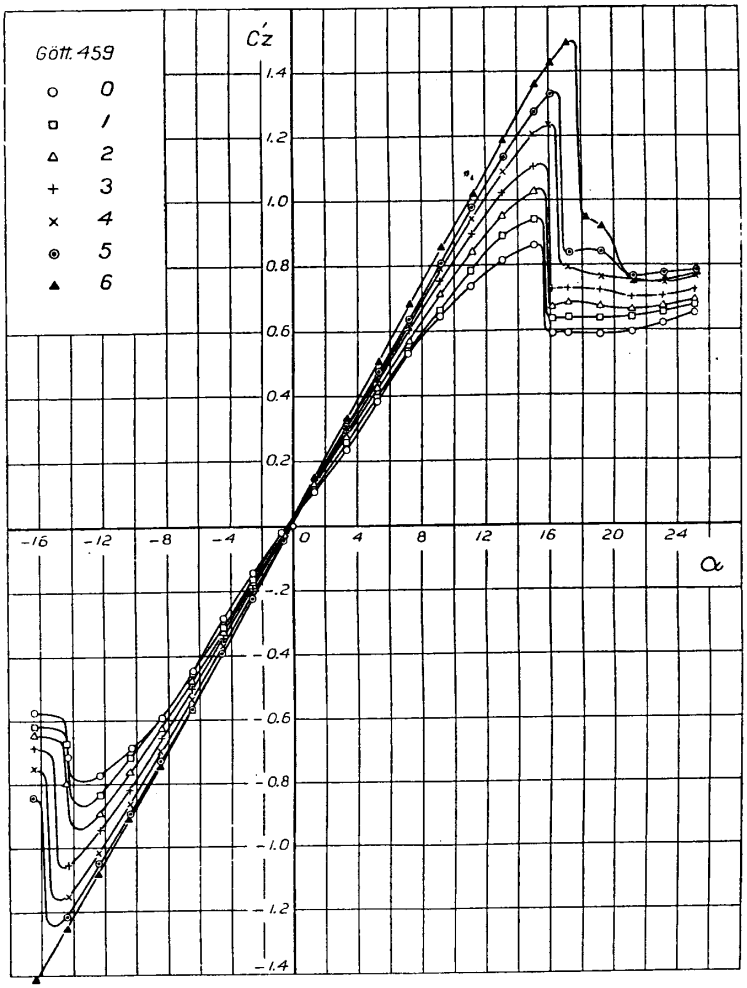

Fig. 55. Curves of the lift coefficient based on the actual wing area.

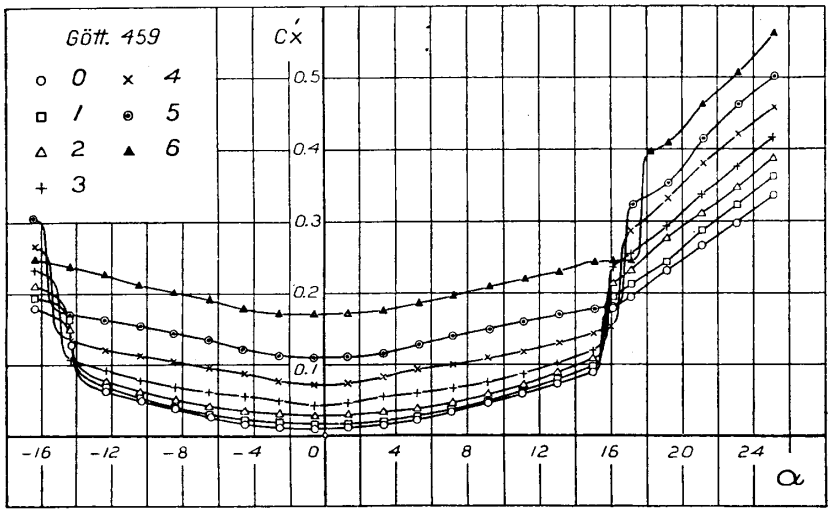

Fig. 56. Curves of the drag coefficient based on the actual wing area.

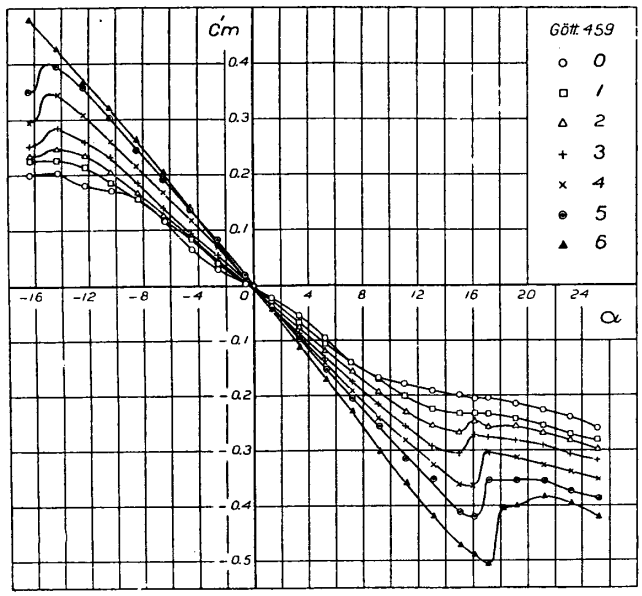

Fig. 57. Curves of the moment coefficient based on the actual wing area and chord length.

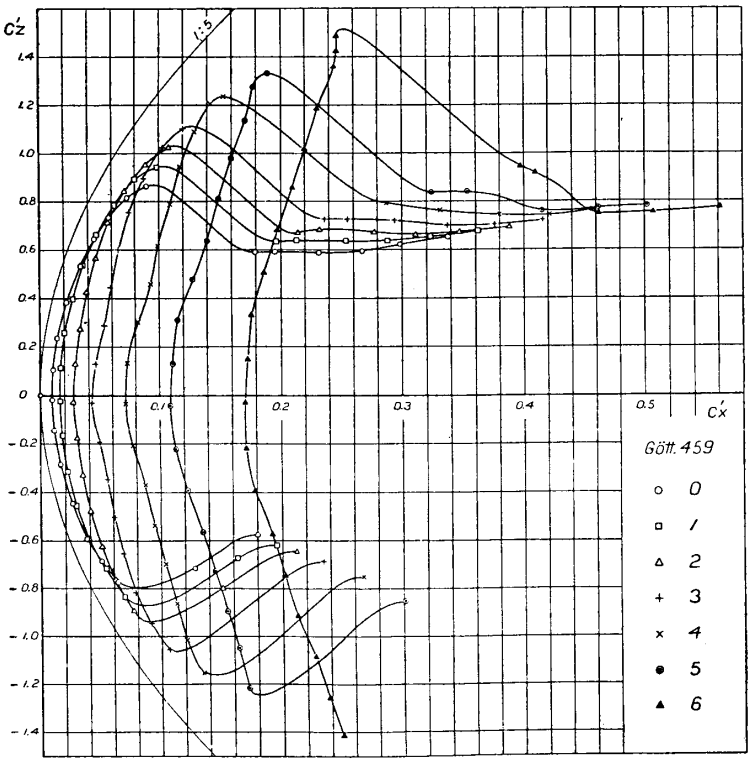

Fig. 58. Polar curves. The coefficients are based on the actual wing area.

II. *The cut end is made round with the inscribed circle.*

Next, the tests were made with ragard to the case in which the cut end is made round with the inscribed circle. The model wings are shown in Fig. 59, and the results of the tests are shown in figures from 65 to 74.

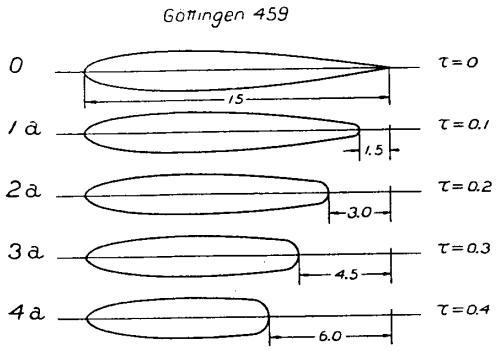

Fig. 59. The model wings. The span is 75 cm for all wings.

(i) *Lift coefficient.* The lift coefficient based on the original wing area is plotted against the angle of incidence in Fig. 65. The variation of the curve of the lift coefficient with the depth of cut-out has, on the whole, the same tendency as for the case in which the cut end is not made fair, and the lift curves for these two cases are compared in detail in Fig. 6. It indicates that if the cut end is made round with the inscribed circle the maximum lift coefficient decreases

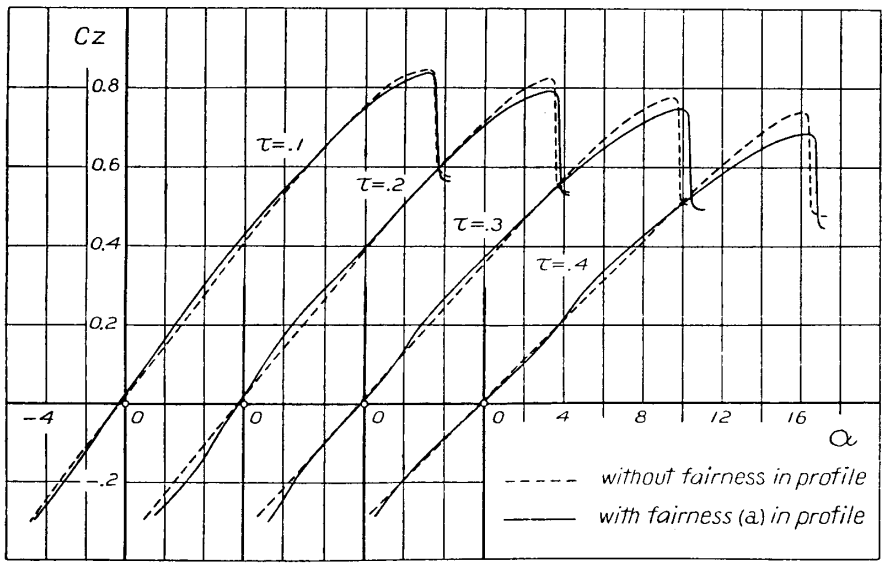

Fig. 60. Comparison of the curve of the lift coefficient of the wing whose cut end is made round with that of the wing whose cut end is not made fair.

and the stalling angle increases in comparison with the case in which the cut end is not made fair, the local increase of the lift coefficient occurring at small angles of incidence. The decrease of the maximum lift coefficient with τ is shown in Fig. 61.

The lift coefficient based on the actual wing area is plotted against the angle of incidence in Fig. 71. Both the value of $\frac{dc_z}{d\alpha}$ and the maximum lift coefficient increase with the depth of cut-out, similarly as for the Göttingen 593 wing.

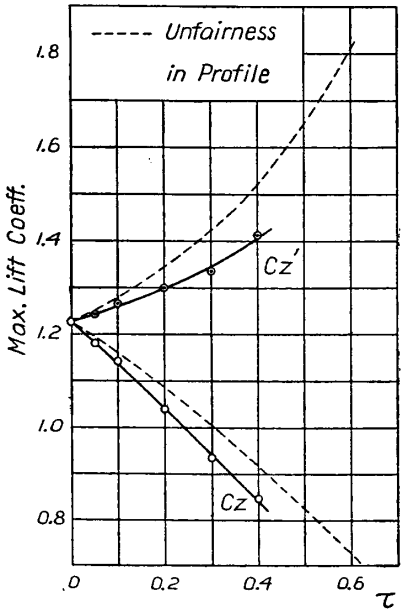

Fig. 61. Variation of the maximum lift coefficient with the depth-chord ratio τ. c_z is based on the original wing area, and c_z' based on the actual one.

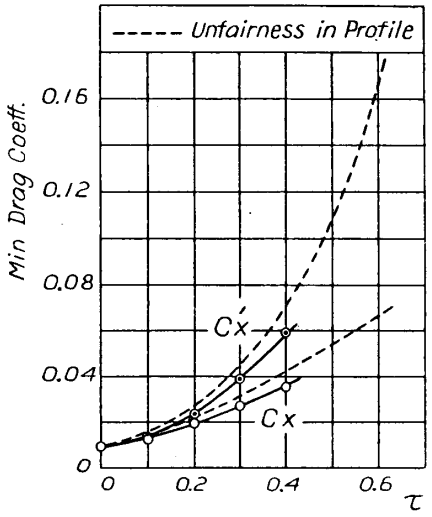

Fig. 62. Variation of the minimum drag coefficient with the depth-chord rotio τ. c_x is based on the original wing area, and c_x' based on the actual one.

(ii) *Drag coefficient.* The variation of the curves of the drag coefficient plotted against the angle of incidence with the depth of cut-out has, on the whole, the same tendency as for the case in which the cut end is not made fair, but the values of the drag coefficient decreases, of course, considerably throughout all angles of incidence. The minimum drag coefficient increases with τ as shown in Fig. 62.

The drag coefficient based on the actual wing area is plotted against the angle of incidence in Fig. 72.

(iii) *Moment coefficient and centre of pressure coefficient.* The moment coefficient based on the wing area and chord length of the original wing decreases with increasing the depth of cut-out as shown in Fig. 67, and that based on the actual ones increases on the contrary, as is shown in Fig. 73.

The centre of pressure coefficient based on the original chord length decreases with increasing the depth of cut-out as shown in Fig. 68. And the variation of this coefficient at $+10^\circ$ angle of incidence with τ, which is shown in Fig. 63, coincides quitely with that for the case in which the cut end is not made fair.

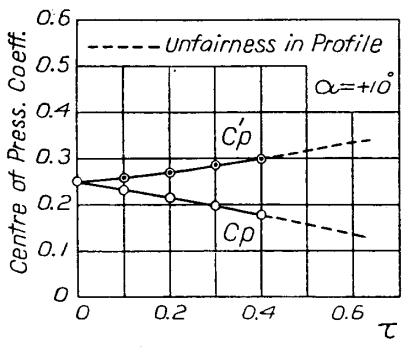

Fig. 63. Variation of the centre of pressure coefficient at $+10^\circ$ angle of incidence with the depth-chord ratio τ. c_p is based on the original chord length, and c_p' based on the actual one.

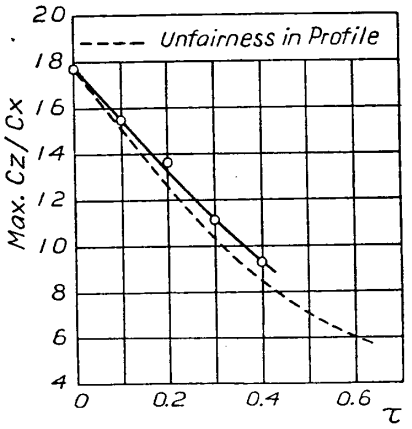

Fig. 64. Variation of the maximum value of the lift-drag ratio with the depth-chord ratio τ.

(iv) *Lift-drag ratio.* The lift-drag ratio is plotted against the angle of incidence in Fig. 69. The variation of the lift-drag ratio with τ has, on the whole, the same tendency as for the case in which the cut end is not made fair, but the value of this ratio decreases strongly. The variation of the maximum value of the ratio c_z/c_x with τ is plotted in Fig. 64. The angle of incidence at which the maximum value of the ratio c_z/c_x occurs is for this case greater than for the case in which the cut end is not made fair.

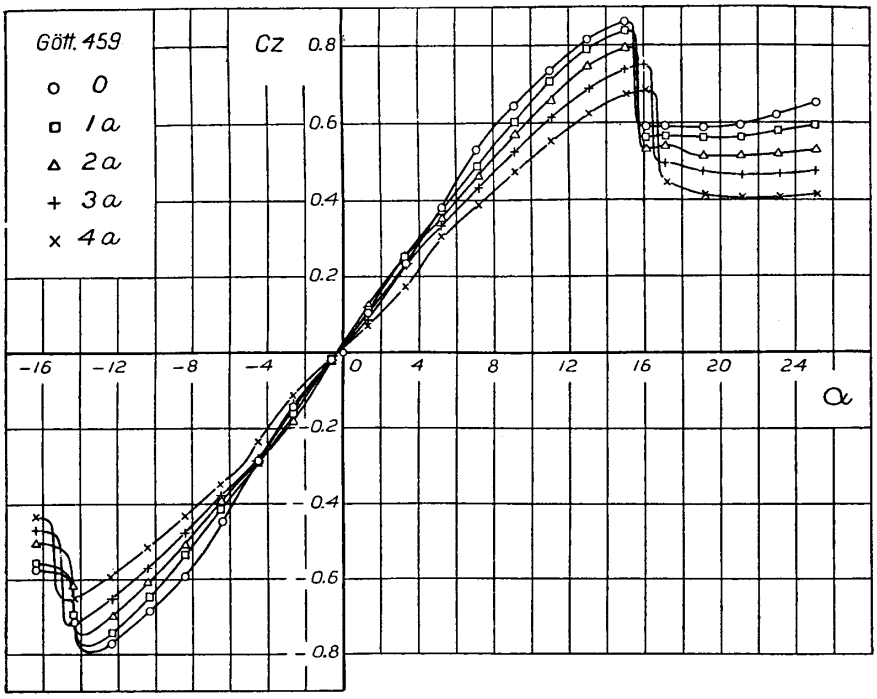

Fig. 65. Curves of the lift coefficient based on the original wing area.

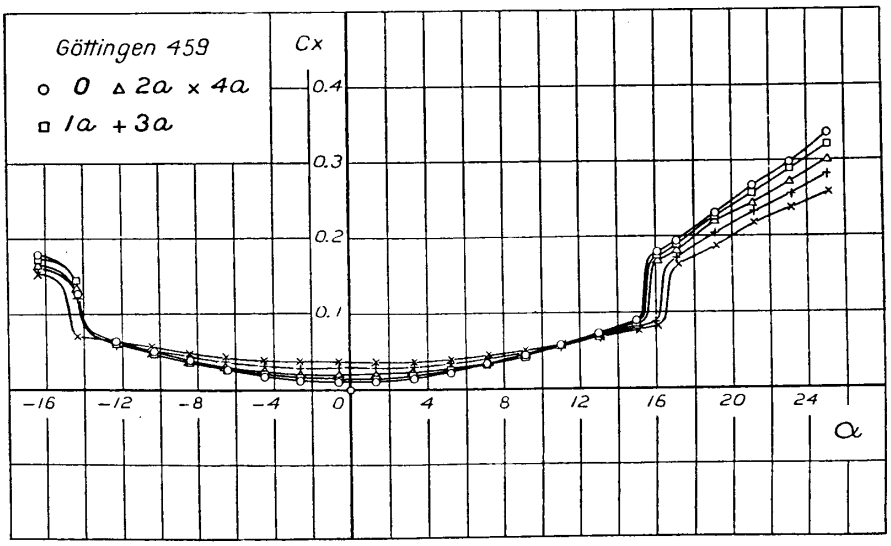

Fig. 66. Curves of the drag coefficient based on the original wing area.

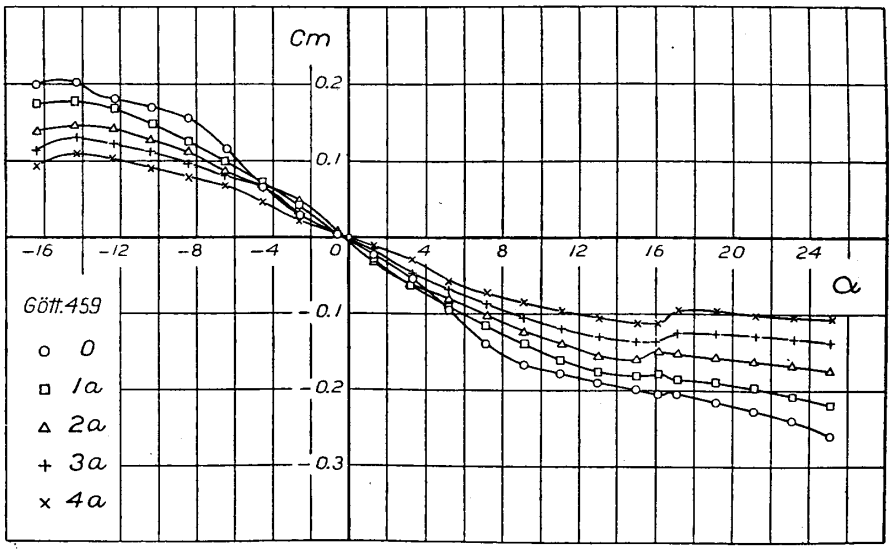

Fig. 67. Curves of the moment coefficient based on the wing area and chord length of the original wing.

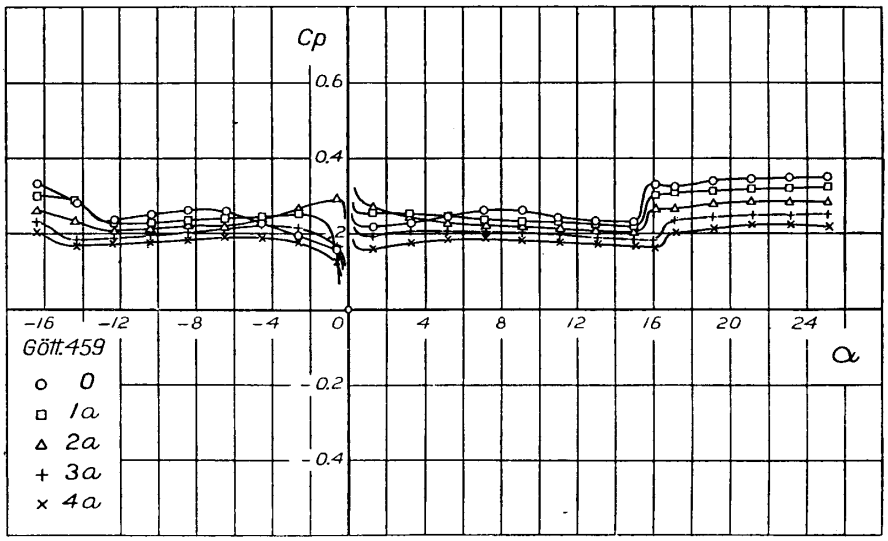

Fig. 68. Curves of the centre of pressure coefficient based on the chord length of the original wing.

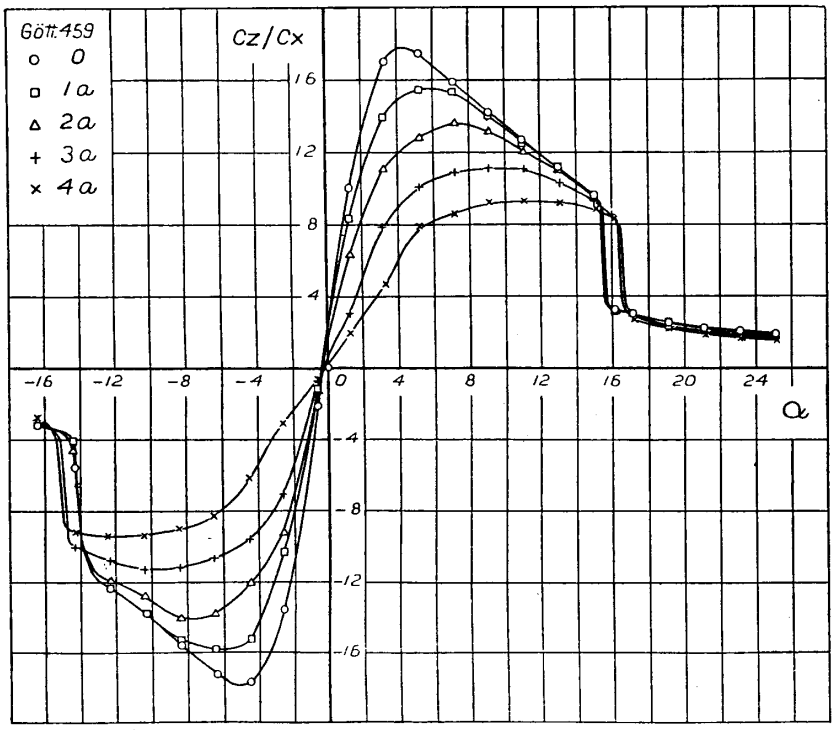

Fig. 69. Curves of the lift-drag ratio.

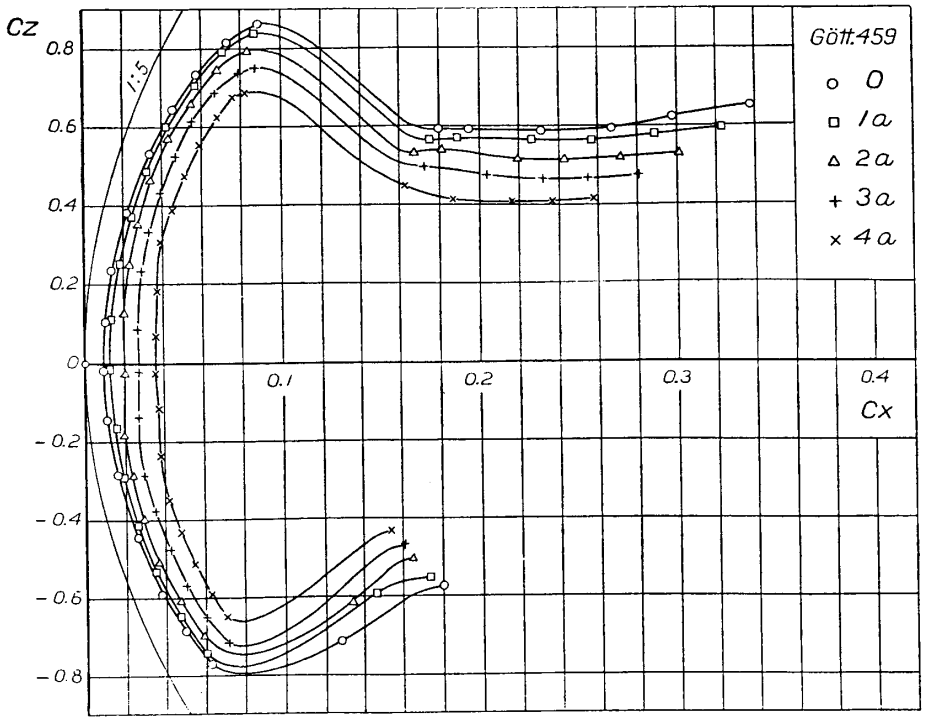

Fig. 70. Polar curves. The coefficients are based on the original wing area.

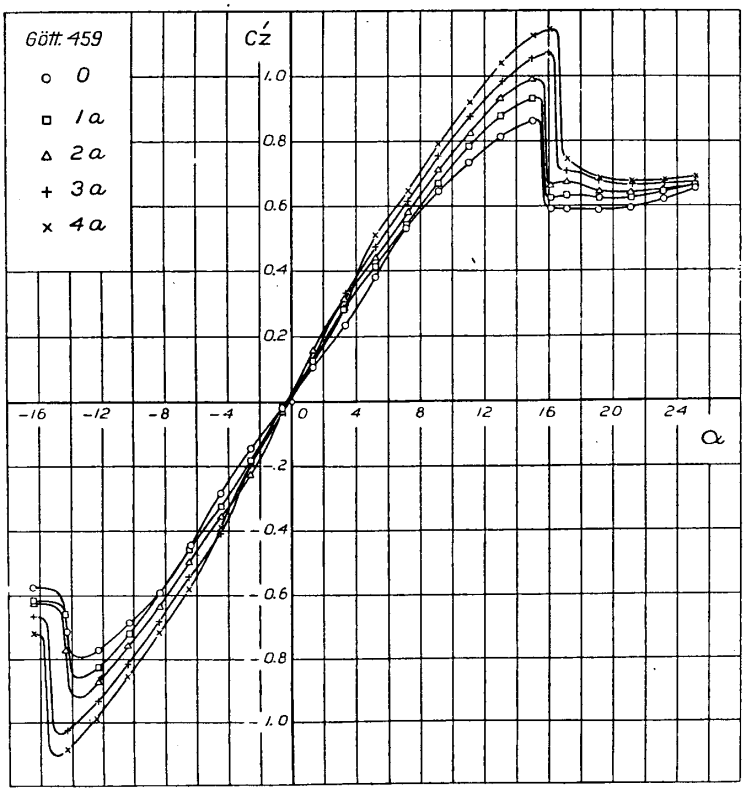

Fig. 71. Curves of the lift coefficient based on the actual wing area.

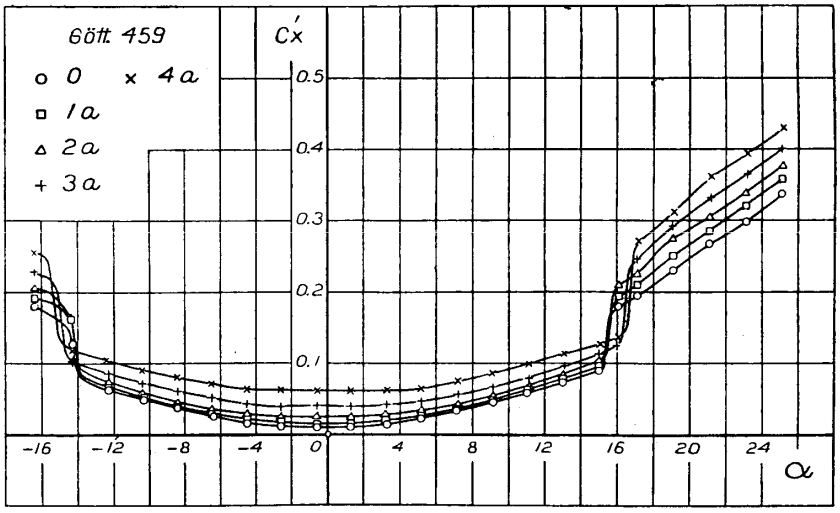

Fig. 72. Curves of the drag coefficient based on the actual wing area.

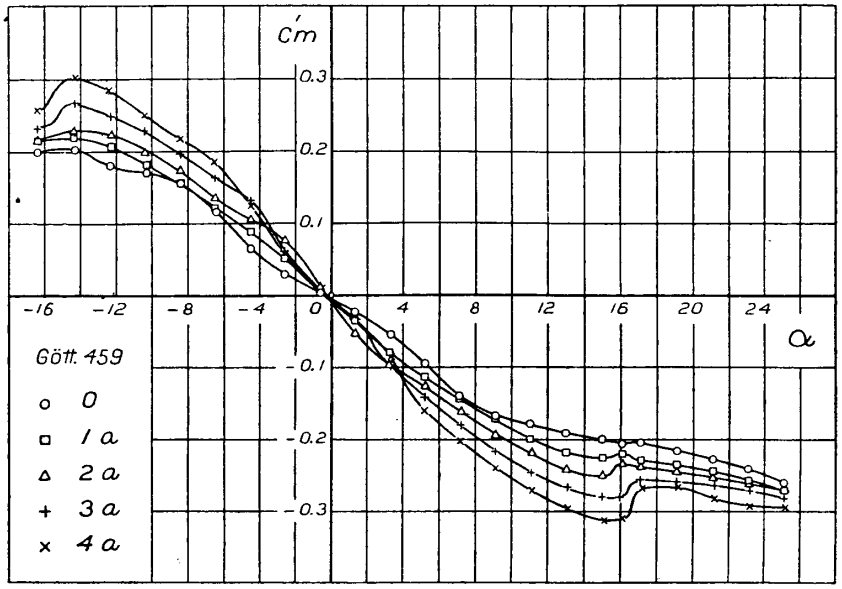

Fig. 73. Curves of the moment coefficient based on the actual wing area and chord length.

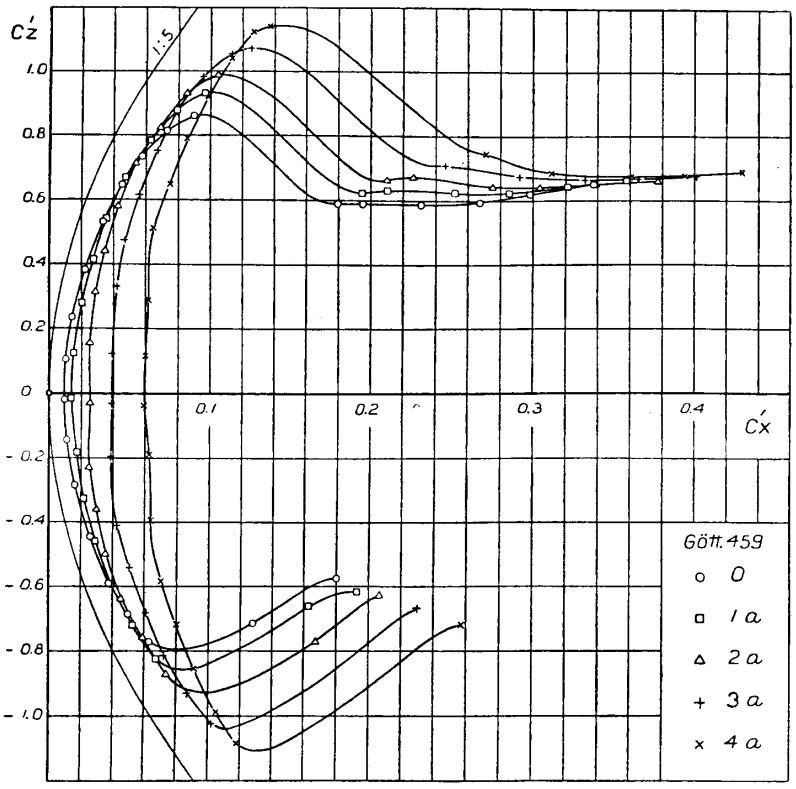

Fig. 74. Polar curves. The coefficients are based on the actual wing area.

III. *Comparison of the characteristics of the wings with various cutaway sections.*

From the preceding two tests the difference between the characteristics of the wing without fairness in the cut end and those of the whose cut end is made round with the inscribed circle could be known. Now, we shall test the characteristics of the wings whose cutaway sections are designated by $3b$ and $3c$ in Fig. 75 with regard to the case of $\tau = 0{\cdot}3$, and from these results we shall choose the most suitable section in the four sections shown in Fig. 75. The results of the tests are plotted in curves in figures from 79 to 84.

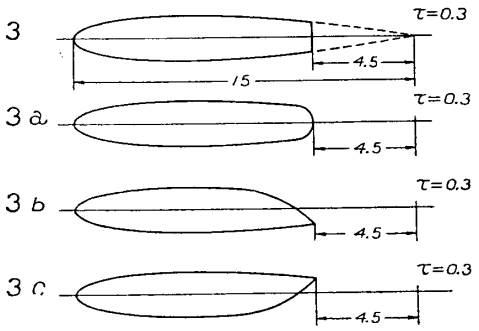

Fig. 75. The model wings. The span is 75 cm for all wings.

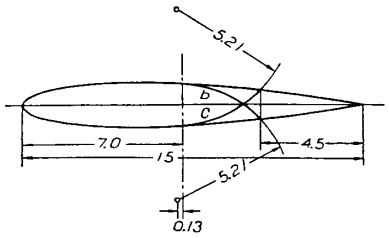

Fig. 76. Details of the $3b$ and $3c$ wings.

(i) *Lift coefficient.* As the present tests were made for purpose of comparing the characteristics of the wings of various cutaway sections, the discussion on the results was done regarding only the aerodynamic coefficients based on the dimensions of the original wing.

The lift coefficient is plotted against the angle of incidence in Fig. 79. The tendency of the variation of the curve of the lift coefficient with the cutaway section is, on the whole, similar to that of the Göttingen 593 wing. The variation of the zero lift angle with the cutaway section is so small that it can be approximately neglected.

The lift coefficient of the "$3b$" wing increases so strongly at angles of incidence from about 2° to 10° that a protuberance occurs on the

lift curve at this range of angle of incidence. The maximum lift coefficient of this wing is somewhat smaller than for the "3*a*" wing.

The lift coefficient of the "3*c*" wing is smaller than for the other wings, and hence the maximum lift coefficient for this wing is smaller than for other wings.

The comparison of the values of the maximum lift coefficient of these wings is illustrated in Fig. 77.

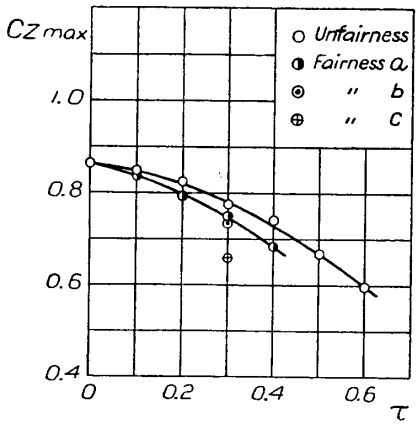

Fig. 77. Variation of the maximum lift coefficient with the fairness in the cut end, plotted against the depth-chord ratio τ.

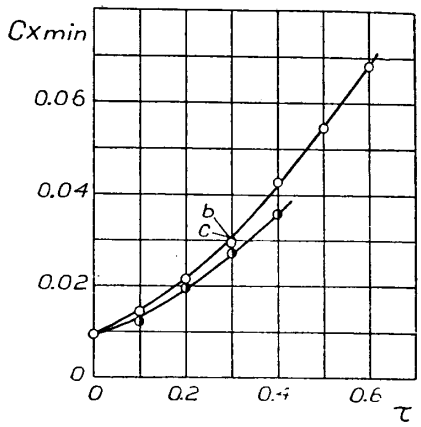

Fig. 78. Variation of the minimum drag coefficient with the fairness in the cut end, plotted against the depth-chord ratio τ.

(ii) *Drag coefficient.* The drag coefficient is plotted against the angle of incidence in Fig. 80. The variation of the drag coefficient with the cutaway section is not so large as that of the Göttingen 593 wing. The values of the minimum drag coefficient of these wings are plotted against τ in Fig. 78. Cx_{min} of the "3*b*" and "3*c*" wings are approximately equal to that of the "3" wing whose cut end is not made fair.

(iii) *Moment coefficient and centre of pressure coefficient.* Fig. 81 shows the curves of the moment coefficient plotted against the angle of incidence. The moment coefficient of the "3*c*" wing is smallest in the

four wings, and in the case of the "3 *b*" wing the moment curve has a protuberance at angles of incidence from 2° to 10°, similarly as in the lift curve.

The centre of pressure coefficient is plotted against the angle of incidence in Fig. 82. The centre of pressure coefficient of the "3 *b*" wing is larger than for the other wings, which indicates that the air forces on the portion near the trailing edge increases in this case, and it varies considerably with the angle of incidence.

If the cut end is made fair with "*c*" type, the air forces on the portion near the trailing edge seems to decrease.

(iv) *Lift-drag ratio.* The lift-drag ratio is plotted against the angle of incidence in Fig. 83. From the standpoint of the maximum value of the lift-drag ratio the fairness of "*b*" type is most desirable and the fairness of "*a*" type is secondly efficient.

(v) *Conclusions.* If the cut end is rounded with the inscribed circle, the maximum lift coefficient somewhat decreases still more and at small angles of incidence the lift coefficient does approximately not differ in comparison with the case in which the cut end is not made fair. And in this case the drag coefficient decreases strongly, which leads to the increase of the lift-drag ratio.

If the cut end is made fair with "*b*" type, the drag coefficient decreases, and the lift coefficient increases considerably at the angles of incidence from 2° to 10° as compared with the case in which the cut end is not made fair. And thus the lift-drag ratio increases considerably in this range of the angle of incidence.

When the cut end is made fair with "*c*" type, the lift coefficient decreases and the other characteristics are also unsatisfactory.

From the above discussions it is concluded that the fairness of "*a*" type must be chosen for the cutaway section of the wing with cut-out in the four types tested, although the fairness of "*b*" type gives locally some satisfactory characteristics.

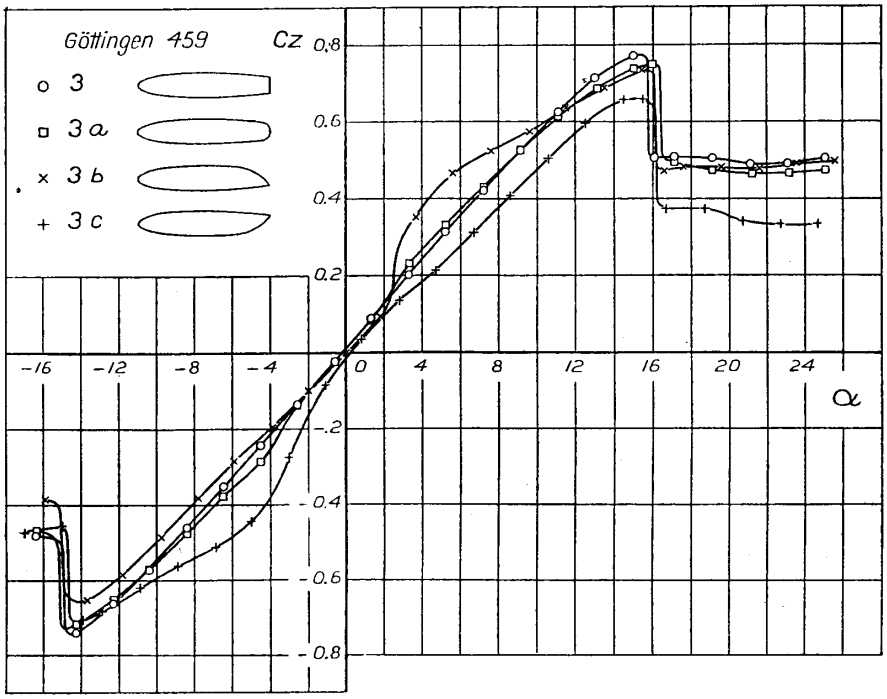

Fig. 79. Curves of the lift coefficient.

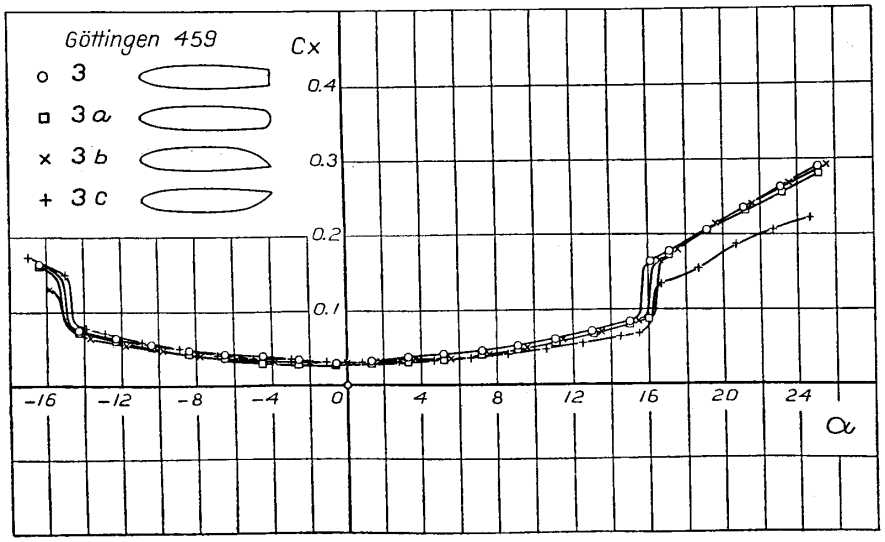

Fig. 80. Curves of the drag coefficient.

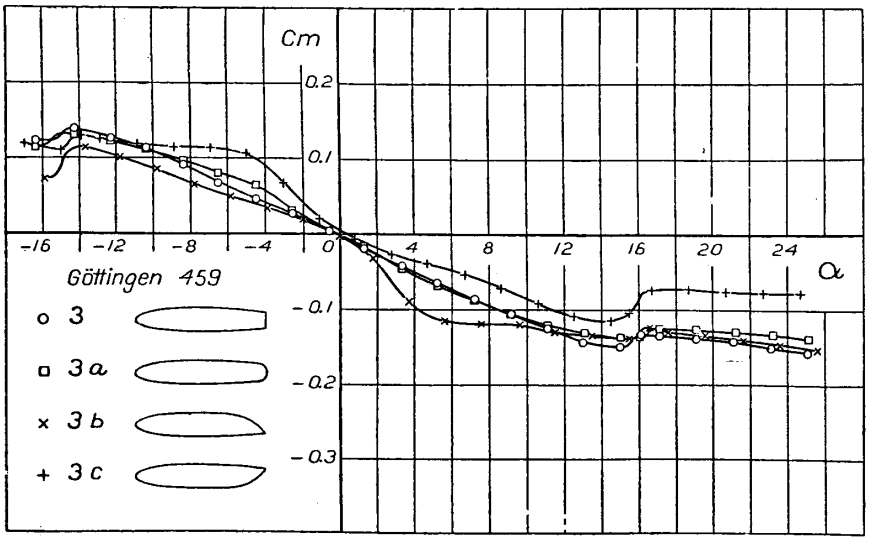

Fig. 81. Curves of the moment coefficient.

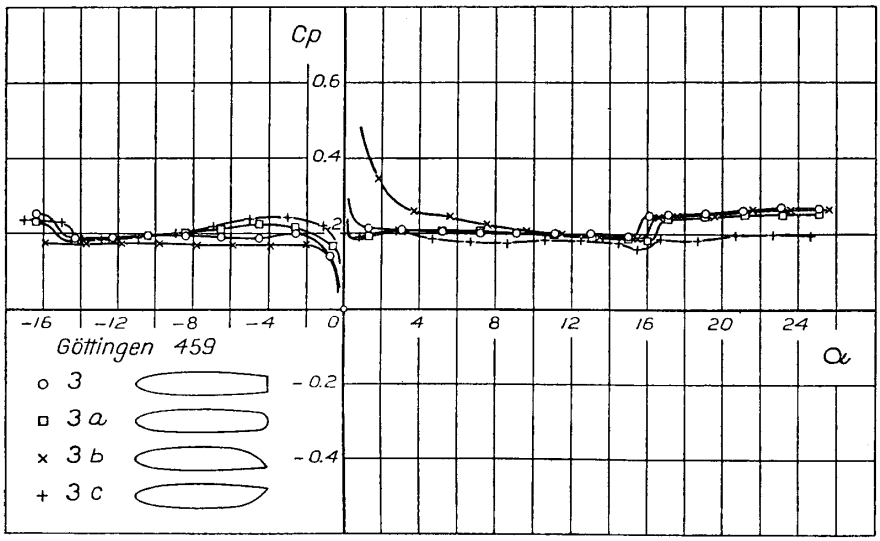

Fig. 82. Curves of the centre of pressure coefficient.

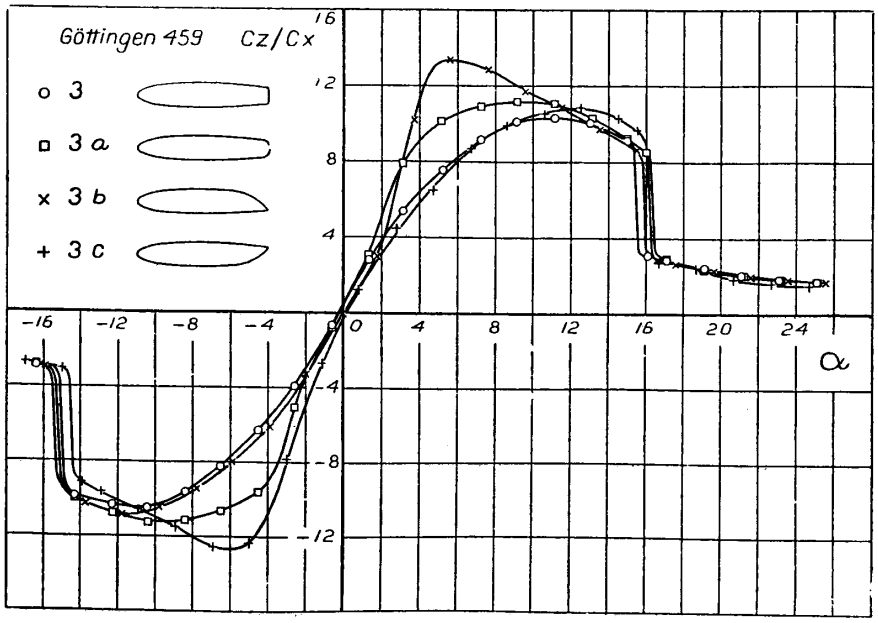

Fig. 83. Curves of the lift-drag ratio.

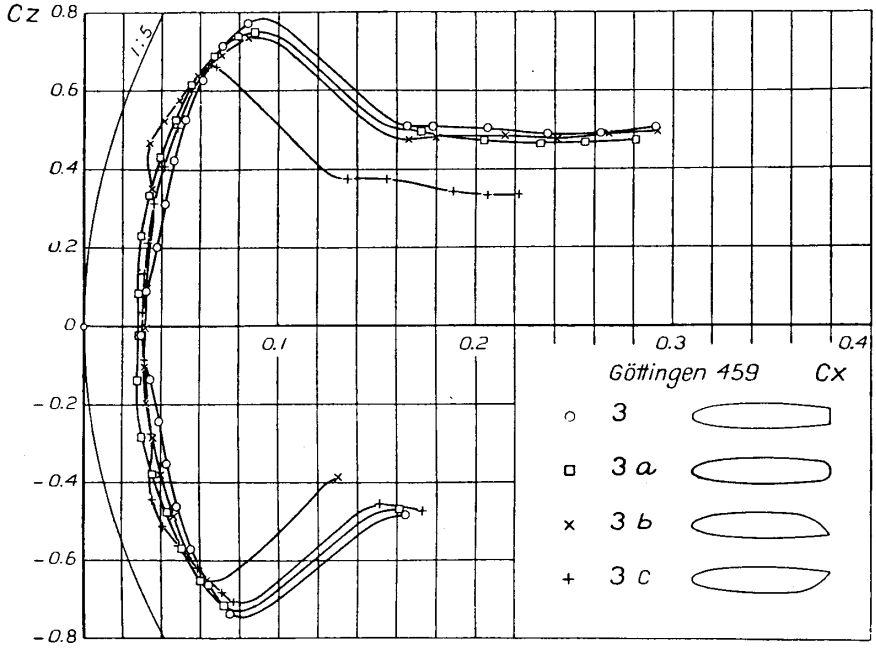

Fig. 84. Polar curves.

6. A theoretical discussion on the lift of the wing whose trailing edge is cut away.

From the preceding wind tunnel tests we have known that if the trailing edge is cut away the lift coefficient[7] decreases, the rate of which depends strongly on the camber of profile, and the slope of the curve of the lift coefficient plotted against the angle of incidence also decreases, the rate of which is independent of the camber of profile. And in the case of the non-cambered profile or the symmetrical profile the angle of zero lift does not be altered with cutting the trailing edge, but for the cambered profile it decreases with the depth of cut-out.

Now, we shall discuss theoretically such properties which are dependent on the camber of profile, confining the problem to the thin wing in two dimensions. And for the sake of simplicity of consideration we shall represent the cambered wing by the circular arc, and the non-cambered wing by the straight line.

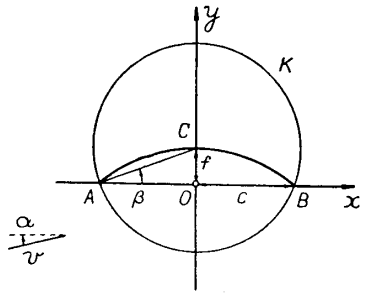

Fig. 85

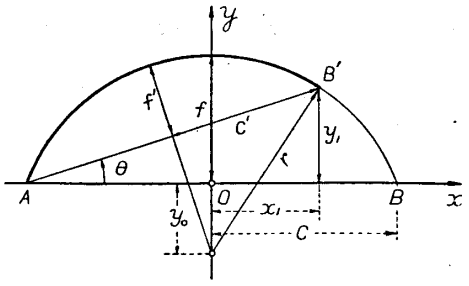

Fig. 86

It is well-known that the circle K whose centre is at the point $z = if$ in the z-plane is transformed into a circular arc ABC in the ξ-plane by the transformation

$$\xi = \frac{1}{2}\left(z + \frac{a^2}{z}\right),$$

(7) It will be taken the lift coefficient based on the original wing area.

where a is the radius of the circle, as is shown in Fig 85. And hence the potential flow around this circular arc can, as is well-known, be obtained from that around the circle. Determining the circulation around the circular arc by the condition that the flow must leave smoothly the trailing edge, then the lift on the circular arc is

$$\bar{F}_z = \pi \rho t v^2 \frac{\sin(\alpha+\beta)}{\cos\beta}\ ,^{(8)}$$

$$= \pi \rho t v^2 \sin\alpha\,(1+\sigma\cot\alpha)\ , \qquad (5)$$

where ρ is the density of air, t the chord length, v the velocity of the flow at infinity, α the angle of incidence, and $\sigma = \frac{f}{c} = 2\frac{f}{t}$.

In the case of the circular arc the cutaway section is still a circular arc whose maximum camber decreases to f', the chord length to t', and the effective angle of incidence[9] becomes $\alpha' = \alpha - \theta$, where θ is the angle between AB and AB' as is shown in Fig. 86. Hence the lift of the wing whose trailing edge is cut away becomes

$$F_z = \pi \rho t' v^2 \sin\alpha'\,(1+\sigma'\cot\alpha') \qquad (6)$$

Next, we shall express σ', α' and t' as the functions of σ and t of the original wing and τt the depth of cut-away.

The equation of the circular arc is $x^2+(y+y_0)^2 = r^2$,

where $y_0 = c\frac{1-\sigma^2}{2\sigma}$ and $r = c\frac{1+\sigma^2}{2\sigma}$.

From Fig. 86 we have $y_1 = \sqrt{r^2-x_1^2} - y_0$.

---

(8) See R. GRAMMEL, Die hydrodynamischen Grundlagen des Fluges. S. 73.

(9) The effective angle of incidence is used in this case to mean the angle between the line connecting the leading edge with the trailing edge of the mean camber line and the direction of flow.

Denoting the ratio of the depth of cut-out to the chord length with τ, then $\tau = \frac{c-x_1}{2c}$. Therefore, we have $x_1 = c(1-2\tau)$.

Hence $$y_1 = \frac{c}{2\sigma}\left[\sqrt{(1-6^2)^2+16\sigma^2\tau(1-\tau)}-(1-\sigma_2)\right] \equiv \frac{c}{2\sigma}\varphi ,$$

where $$\varphi = \sqrt{(1-\sigma^2)^2+16\sigma^2\tau(1-\tau)}-(1-\sigma^2) . \qquad (7)$$

The angle θ between AB and AB' is

$$\theta = tg^{-1}\frac{y}{c+x_1} = tg^{-1}\frac{\varphi}{4\sigma(1-\tau)} .$$

Therefore, $$\alpha' = \alpha-\theta = \alpha-tg^{-1}\frac{\varphi}{4\sigma(1-\tau)} . \qquad (8)$$

The chord length $t' = 2c'$ and the maximum camber f' of the wing whose trailing edge is cut away are written in the forms

$$2c' = 2c(1-\tau)\sec\theta , \qquad f' = r-\sqrt{r-c'^2} .$$

Hence $$\sigma' = \frac{f'}{c'} = \psi-\sqrt{\psi^2-1} ,$$

where $$\psi = \frac{r}{c'} = \frac{(1+\sigma^2)\cos\theta}{2\sigma(1-\tau)} . \qquad (9)$$

And $$\frac{t'}{t} = (1-\tau)\sec\theta \qquad (10)$$

The values of θ and σ' are shown as the functions of τ in Figs. 87 and 88, respectively. And these curves may be considered to be the straight lines, as is seen in the figures.

Substituting the values of α', σ' and t'/t expressed by the equations (8), (9) and (10) into the equation (6), we can calculate the lift on the wing whose trailing edge is cut away.

When the angle of incidence and the camber of profile are small, we can obtain the approximate formula. In such a case we have sin

$\alpha \fallingdotseq \alpha$, $\cos \alpha \fallingdotseq 1$, $t'/t = 1-\tau$ and moreover $\sigma' = \sigma(1-\tau)$, $\theta = m\sigma\tau$ as is seen in Figs. 87 and 88, where $m = 1{\cdot}982$ when θ is in radian.

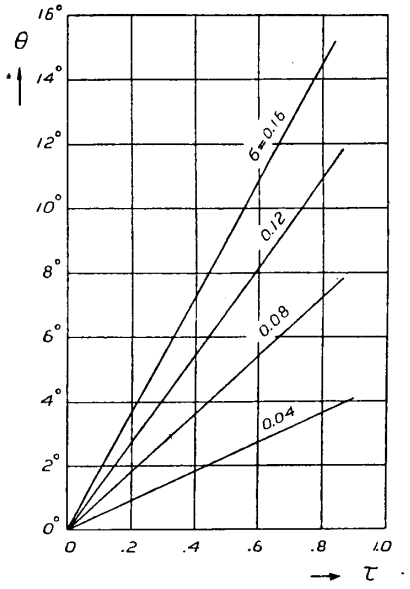

Fig. 87

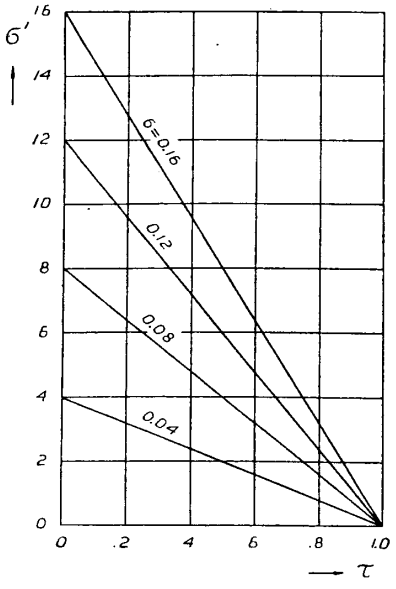

Fig. 88

Therefore, the lift coefficient of the original wing is

$$\bar{c}_z = 2\pi(\alpha+\sigma) \qquad (11)$$

and that of the wing whose trailing edge is cut away is

$$c_z = 2\pi \frac{t'}{t}(\alpha'+\sigma') ,$$

basing on the wing area of the original wing.

Hence, from the above two equations we have

$$c_z = \left[\bar{c}_z - \frac{\bar{c}_z}{\alpha+\sigma}(\theta+\sigma-\sigma')\right]\frac{t'}{t} .$$

Let $\bar{c}_{z_0} = 2\pi\sigma$ or $\bar{c}_{z_0}$ denotes the lift coefficient of the original wing at 0° angle of incidence. Then we have

$$c_z = \left[\bar{c}_z - \bar{c}_{z_0}\left(1 - \frac{\sigma' - \theta}{\sigma}\right)\right]\frac{t'}{t} ,$$
$$= \left[\bar{c}_z - (1+m)\,\tau\,\bar{c}_{z_0}\right](1-\tau) . \qquad (12)$$

In the case of the plate wing we have $\bar{c}_{z_0} = 0$, and hence

$$c_z = \bar{c}_z\,(1-\tau) . \qquad (12a)$$

These equations prove that the slope of the curve of the lift coefficient plotted against the angle of incidence decreases with the depth of cut-out, being independent of the camber of profile, and the zero lift angle does not be altered with cutting the trailing edge for the non-cambered wing, but it decreases for the cambered wing.

The equation (12) is also written in the following form

$$c_z = \left[\bar{c}_z - n\,\bar{c}_{z_0}\right]L_{(\tau)} . \qquad (13)$$

It is to be noticed that this equation (13) is of the same form as the empirical formula (4) which has been established with regard to the Göttingen 593 wing in the limit of $\tau \leqq 0{\cdot}5$, although the aspect ratio is unequal for the both cases. (see p. 353)

In the empirical formula $\bar{c}_z$ is the lift coefficient for the wing of the aspect ratio of 5, and

$$L_{(\tau)} = 1 - 1{\cdot}55\,\tau^2 + 0{\cdot}45\,\tau^3 ,$$
$$n = 1{\cdot}64\,\tau$$

And the calculated values for the circular arc wing of the infinite length are

$$L_{(\tau)} = 1 - \tau ,$$
$$n = 2{\cdot}982\,\tau .$$

The difference between these quantities depends, of course, on the discrepancies in the thickness of the wing, the shape of the mean camber line, the aspect ratio and the properties of the fluid.

7. Photographs of the flow past the Göttingen 593 wing whose trailing edge is cut away.

The variation of the lift coefficient due to cutting the trailing edge can be divided into the decrease of the value of $dc_z/d\alpha$ and that of the angle of zero lift. The former depends upon the depth of cut-out, being independent of the camber of profile, and the latter depends both upon the depth of cut-out and upon the camber of profile.

The effects of the decrease of the chord length is unavoidable and so we must minimize the decrease of the angle of zero lift as possible. But, since the rear spar is usually placed at 50~60 per cent of the chord length behind the leading edge, it has usually been performed in practice to leave the cutaway section just as the original one is in the range from the leading edge to 50~60 per cent of the chord length.

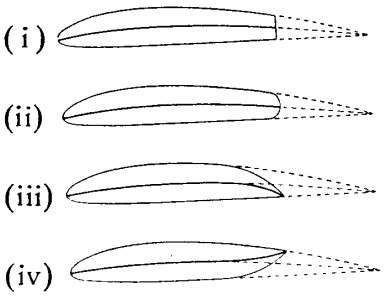

Fig. 89

The cases of (ii), (iii) and (iv) shown in Fig. 89 are the types commonly used to the fairness in the cut end, which have been described in the preceding tests.

If we consider the line of the mean camber in place of the wing section, the camber-chord ratio and the effective angle of incidence for the case of (ii) are equal for (i), and those for (iii) is greater and those for (iv) is smaller than for (i) or (ii). And hence, from the theoretical discussion mentioned above it is expected that the angle of zero lift for (ii) is equal for (i), and that for (ii) is greater and that for (iv) is smaller than for (i). Especially, the angle of zero lift for (iii) is expected to be nearly equal to that of the original wing.

Although this expection is based on the crude assumptions, it is true to some extent as is seen in the experimental results shown in Fig. 90, except the case of (iii) in which the angle of zero lift becomes

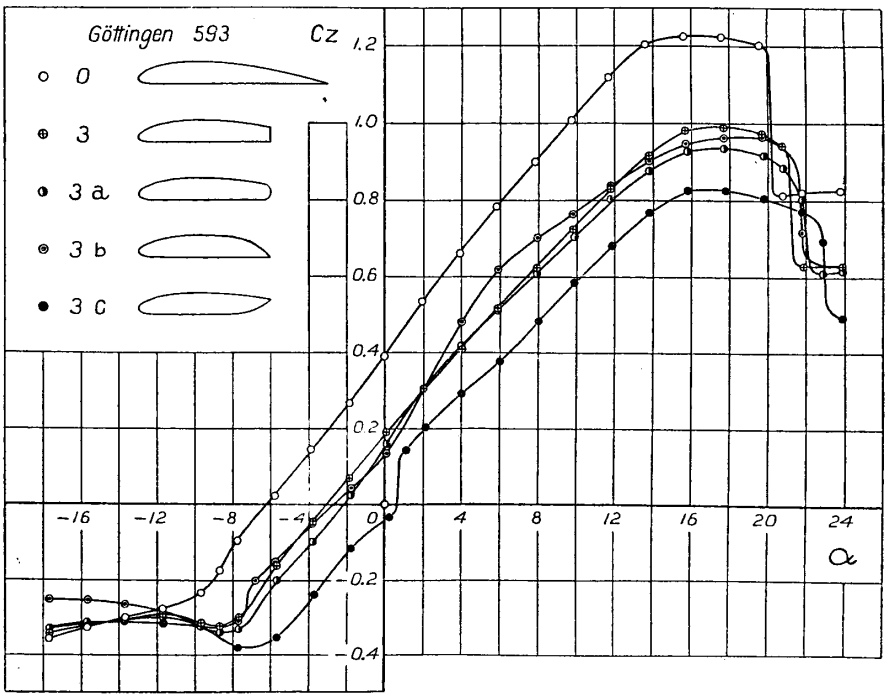

Fig. 90

nearly equal for (i). This disappoint for (iii) must depend on the discrepancy between the assumed flow which leaves smoothly the trailing edge as is designated with (*a*) in Fig. 7 and the actual flow. Namely, it is easily seen that in the actual flow the separation will occur at a point on the upper surface as indicated in Fig. 91 (*b*) because the pressure along the upper surface increases considerably at this place.

(a)

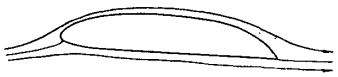

(b)

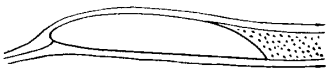

Fig. 91

For purpose of discussing the flow around the wing section whose trailing edge is cut away, the flow patterns have been obtained by photographing the surface of the water in the 30 m × 1·5 m × 1·5 m water tank of the institute after having scattered aluminium powder on it. The camera is mounted on the carriage having the model wing. The velocity of the camera is about 14·7 cm/sec and the chord length

of the original model wing is 40 cm. And the Reynolds' number based on the original chord length is about $0{\cdot}45 \times 10^5$ which is about 15 per cent of that of the wind tunnel tests. The time of exposure of the camera is about 1/10 sec.

The photographs obtained are shown in figures from 92 to 111. It can be seen that, if the trailing edge is cut away, the stall occurs at greater angle of incidence than for the original wing. In the case of (iii) the separation of flow occurs at a point of the upper surface near the rear edge, which must lead to the decrease of the angle of zero lift. In the cases of (ii) and (iv) the wake behind the wing is very small. Especially, in the case of (iv) the region of the wake is considerably small, and hence if the cut end is made fair with this type the tail buffeting and other effects of the wake on the tail surface can be diminished.

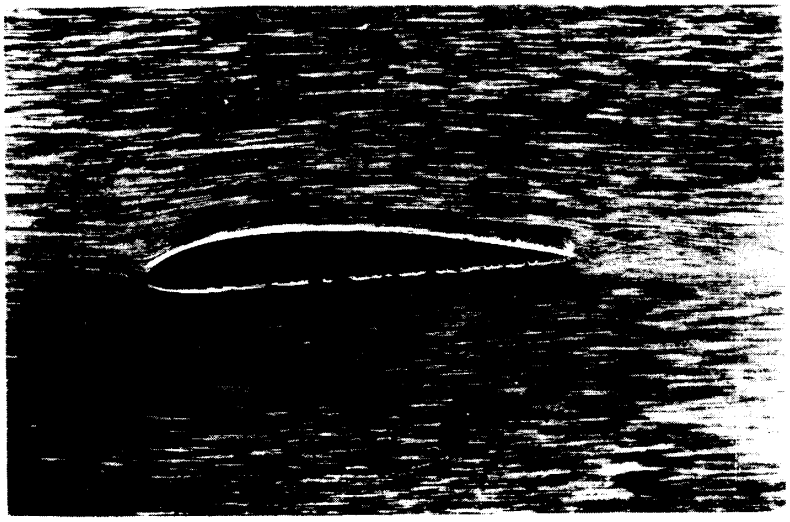

Fig. 92. The normal wing (Göttingen 593). The angle of incidence $\alpha = -6°$, which is nearly equal to the angle of zero lift.

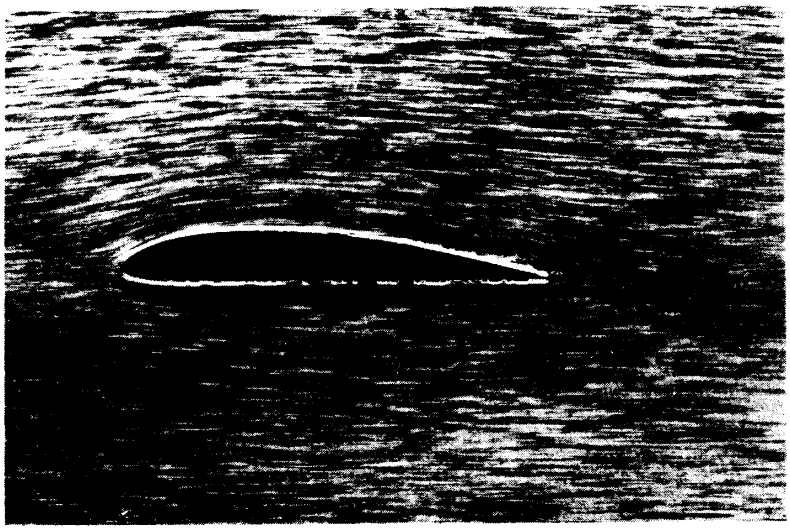

Fig. 93. The normal wing (Göttingen 593). $\alpha = 0°$.

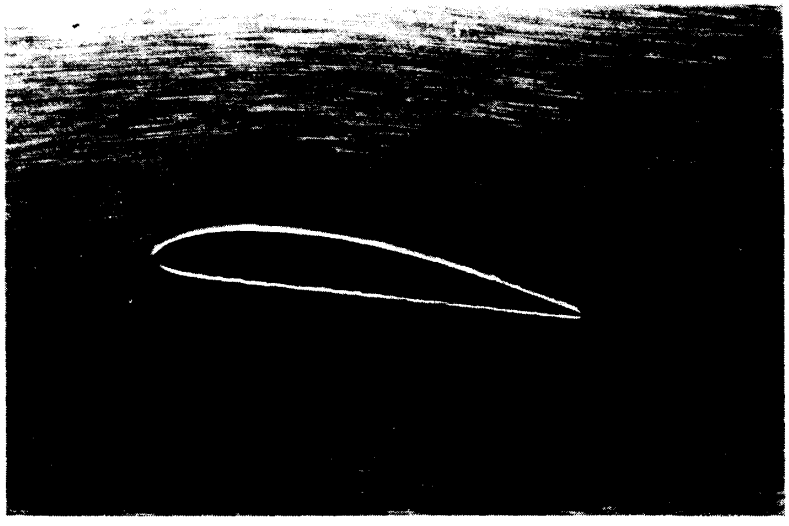

Fig. 94. The normal wing (Göttingen 593). $\alpha = +6°$.
The lift coefficient increases yet with the angle of incidence with the linear relationship.

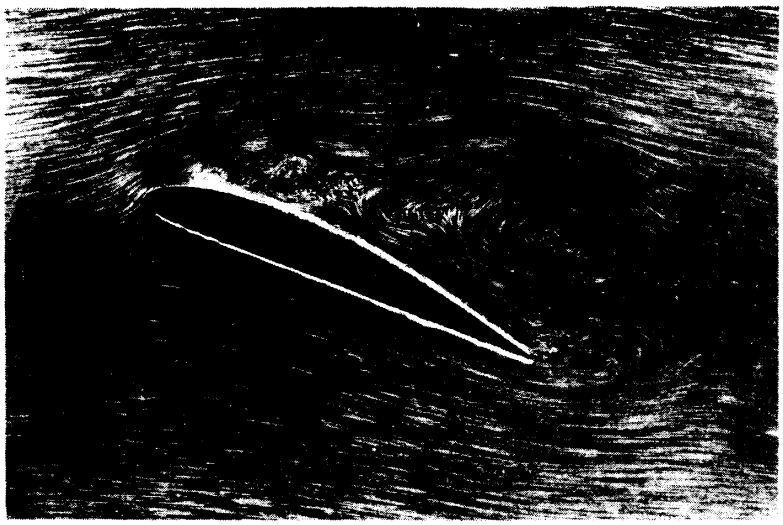

Fig. 95. The normal wing (Göttingen 593). $\alpha = +20°$.
The wing is perfectly in the condition of stall, and the separation of flow occurs near the leading edge.

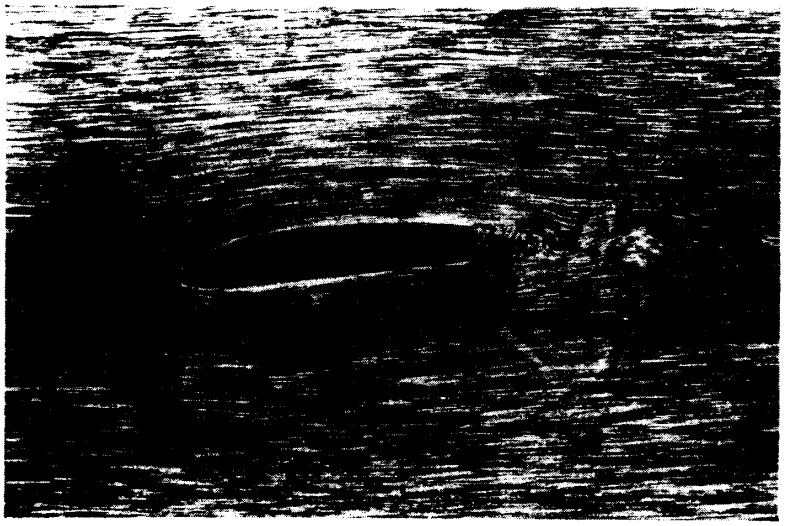

Fig. 96. The "3" wing. $\alpha = -6°$.

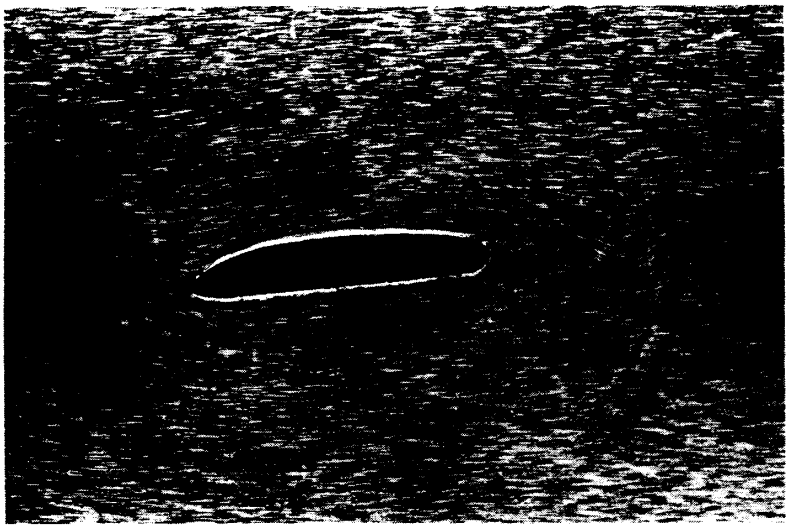

Fig. 97. The "3*a*" wing. $\alpha = -6°$.

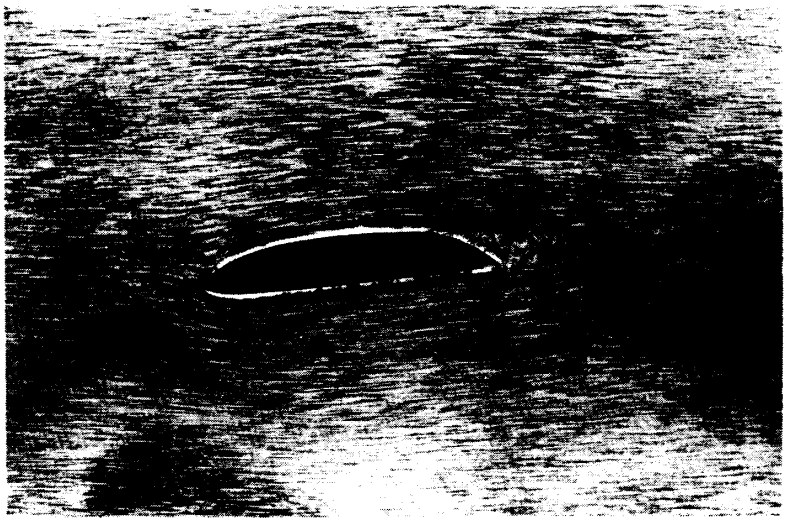

Fig. 98. The "3*b*" wing. $\alpha = -6°$.

Fig. 99. The "3*c*" wing. $\alpha = -6^{\circ}$.

Fig. 100. The "3" wing. $\alpha = 0^{\circ}$.

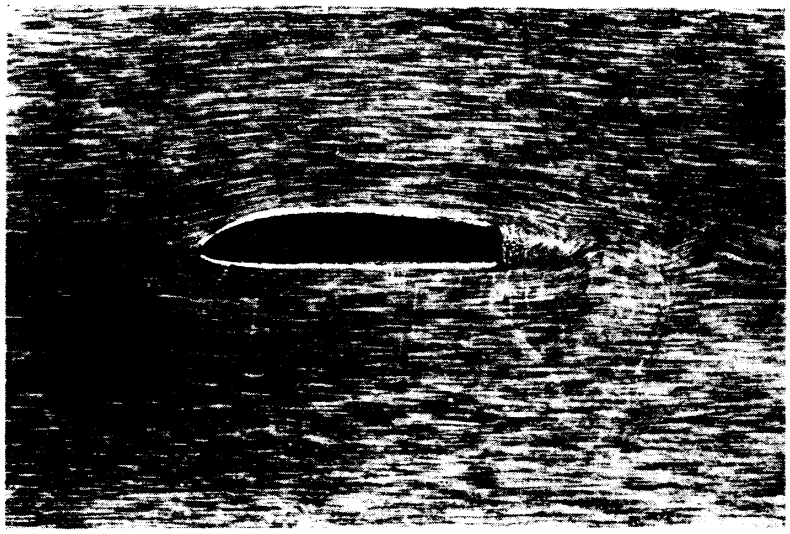

Fig. 101. The "3*a*" wing. $\alpha = 0°$.

Fig. 102. The "3*b*" wing. $\alpha = 0°$.

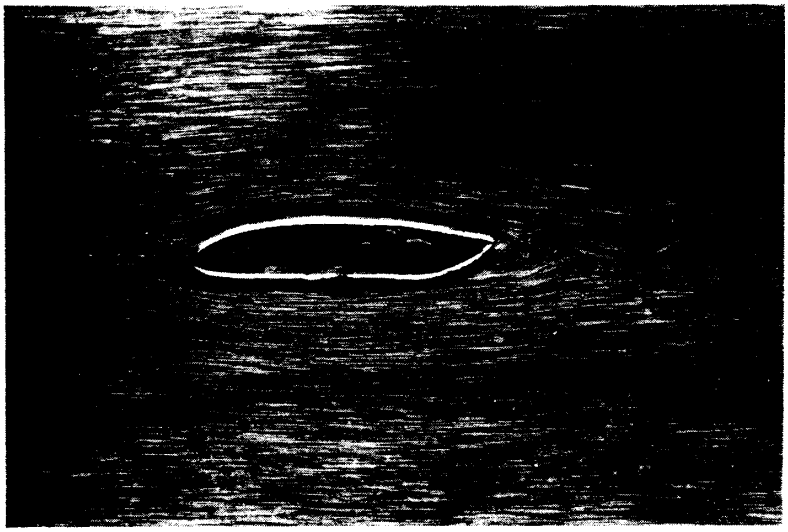

Fig. 103. The "3*c*" wing. $\alpha = 0°$.

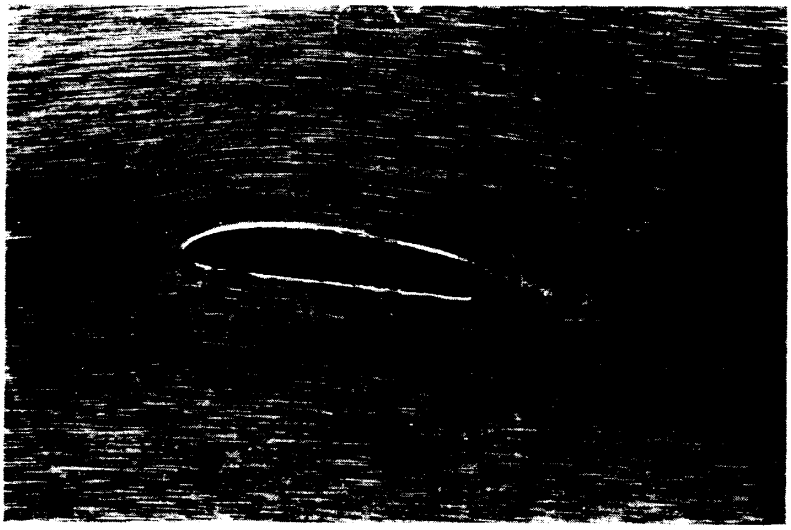

Fig. 104. The "3" wing. $\alpha = +6°$.

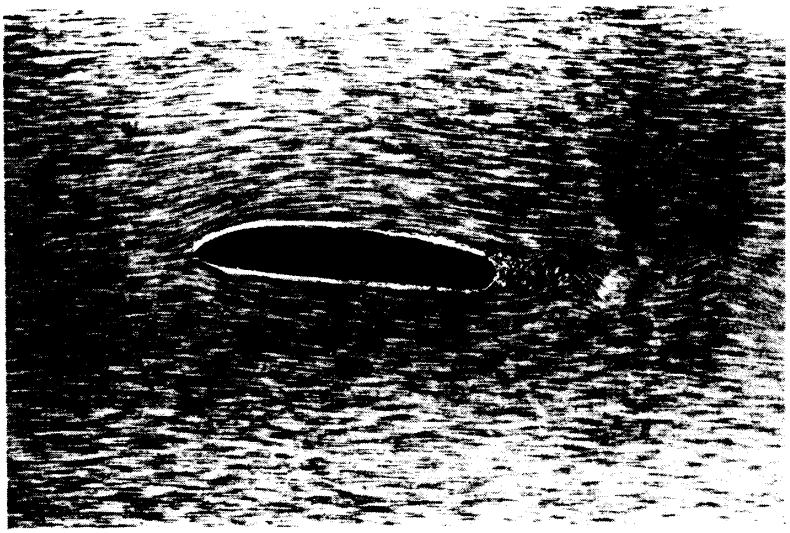

Fig. 105. The "3*a*" wing. $\alpha = +6°$.

Fig. 106. The "3*b*" wing. $\alpha = +6°$.

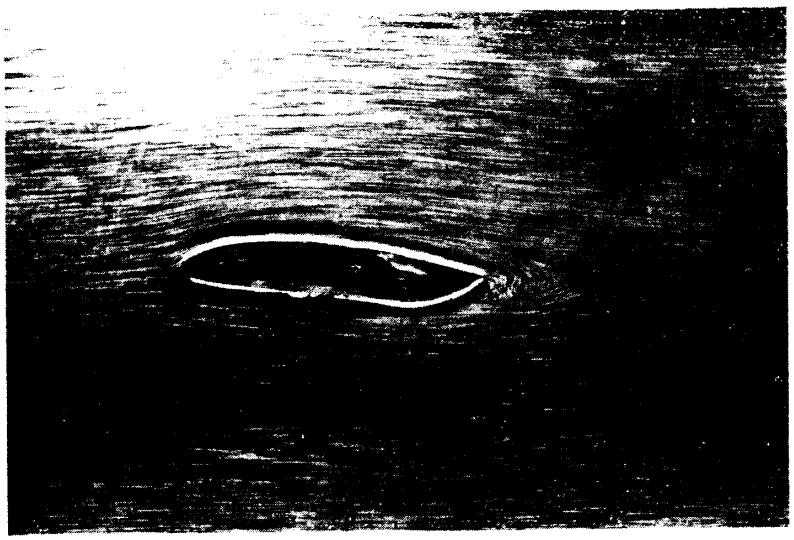

Fig. 107. The "3 *c*" wing. $\alpha = +6°$. The region of the dead water behind the wing decreases considerably compared with the other wings.

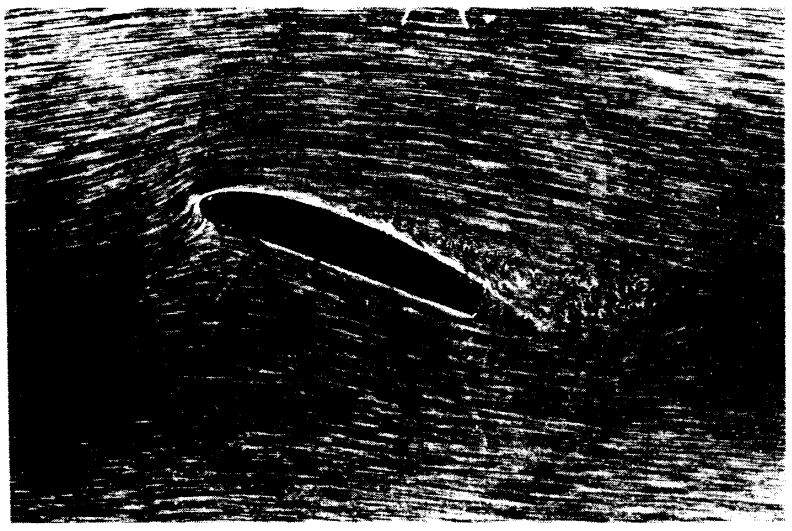

Fig. 108. The "3" wing. $\alpha = +20°$. The wing whose trailing edge is cut away is not yet in the condition of stall, although the original wing is in stall at this angle of incidence.

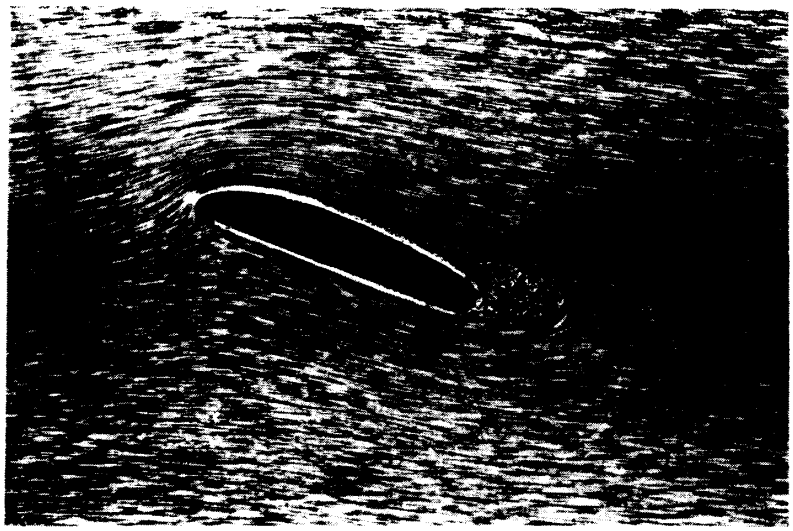

Fig. 109. The "3*a*" wing. $\alpha = +20°$. The region of the dead water behind the wing decreases compared with for the "3" and "3*b*" wings.

Fig. 110. The "3*b*" wing. $\alpha = +20°$. The region of the dead water behind the wing is similar to that of the "3" wing.

Fig. 111. The "3c" wing. $\alpha = +20°$. In this case the wake of the wing is considerably small.

8. Conclusions.

In the case in which the cut end is not made fair, the value of $dc_z/d\alpha$[10] decreases with the depth of cut-out, the rate of decrease being independent of the camber of profile. The angle of zero lift also decreases with the depth of cut-out and the rate of decrease depends much on the camber of profile. Namely, the variation of the angle of zero lift does not occur for the non-cambered profile by cutting the trailing edge. If the trailing edge is cut away, the maximum lift coefficient decreases, and the stall occurs at the greater angle of incidence than for the normal wing. The drag coefficient increases with the depth of cut-out, which leads to the decrease of the ratio of the lift to the drag.

When the cut end is rounded with the inscribed circle, which is in the present report called the "a" type of fairness, the maximum lift coefficient decreases still more compared with the case in which the

(10) The aerodynamic coefficients used in this chapter are based on the wing area of the original wing.

cut end is not made fair, but the lift coefficient at small angle of incidence is not varied so much. The drag coefficient for this case is smaller than for the above case and the wake behind the wing is considerably small.

When the upper corner of the cut end is made fair, which is in the present report called the "*b*" type of fairness, the lift coefficient does not increase and the drag coefficient tends to increase compared with the case in which the cut end is not made fair. And moreover, the wake behind the wing for this case is as great as for the case in which the cut end is not made fair. From these reasons this type of fairness is unsuitable for the cutaway section of the wing with cut-out.

When the lower corner of the cut end is made fair, which is in the present report called the "*c*" type of fairness, the lift coefficient decreases considerably, and the eddy region behind the wing also decreases, which leads to the diminution of the effects of the wake on the tail surface.

But it is impossible to prevent the decrease of the angle of zero lift as long as the types of fairness mentioned above are used. It is seen that the cutaway section must be made similar as the original profile or may be made with the profile of higher camber in order to avoid the decrease of the angle of zero lift.

In conclusion the author wishes to acknowledge his best thanks to Prof. Dr. K. Wada for his cordinal guidance and to Messrs. T. Fukui and K. Yosida for their labour in assisting experiments.

The Wind Tunnel Department,
The Aeronautical Research Institute,
Tokyo Imperial University.
September, 1935.